AD-A129 288 SYNTHESIS OF OPTIMAL DIGITAL CONTROLLER FOR CONTINUOUS-DATA MODEL-FOLLOWING(U) KENTUCKY UNIV LEXINGTON DEPT OF ELECTRICAL ENGINEERING H YEH JAN 83 1/1

UNCLASSIFIED AFOSR-TR-83-0461 AFOSR-82-0207 F/G 12/1 NL

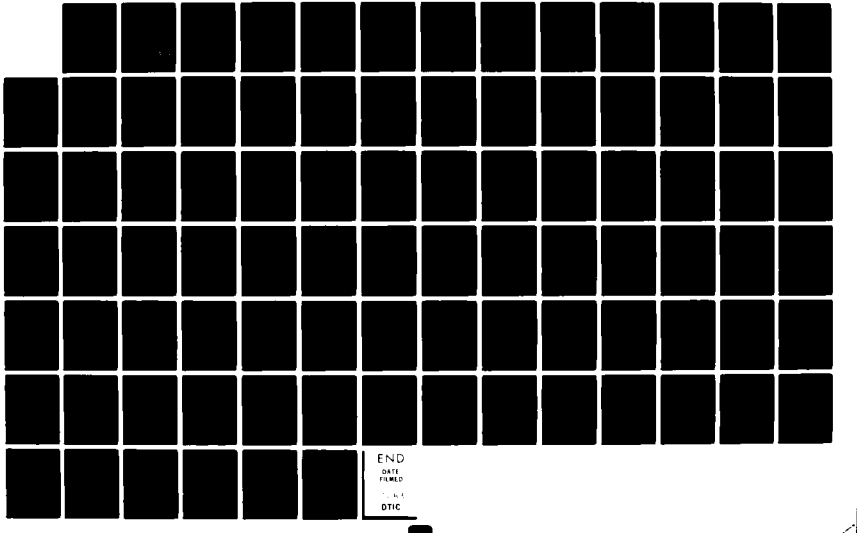

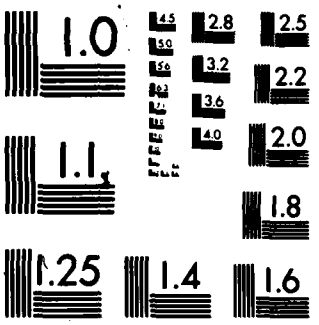

SYNTHESIS OF OPTIMAL DIGITAL CONTROLLER FOR CONTINUOUS-DATA MODEL-FOLLOWING

Grant
~~Report~~ AFOSR-82-0207

SYNTHESIS OF OPTIMAL DIGITAL CONTROLLER FOR CONTINUOUS-DATA MODEL-FOLLOWING

Hsi-Han Yeh
Department of Electrical Engineering
University of Kentucky
Lexington, Ky. 40506

January 1983
Final Report for period MAY 1982 - AUG 1982

Approved for public release : distribution unlimited

Prepared for
AIR FORCE OFFICE OF SCIENTIFIC RESEARCH
BOLLING AIR FORCE BASE
Washington, D.C. 20332

UNCLASSIFIED

SECURITY CLASSIFICATION OF THIS PAGE (When Data Entered)

REPORT DOCUMENTATION PAGE		READ INSTRUCTIONS BEFORE COMPLETING FORM
1. REPORT NUMBER AFOSR-TR- 83-0461	2. GOVT ACCESSION NO. AD-A129288	3. RECIPIENT'S CATALOG NUMBER
4. TITLE (and Subtitle) SYNTHESIS OF OPTIMAL DIGITAL CONTROLLER FOR CONTINUOUS-DATA MODEL-FOLLOWING		5. TYPE OF REPORT & PERIOD COVERED FINAL, 1 MAY 82-31 AUG 82 6. PERFORMING ORG. REPORT NUMBER
7. AUTHOR(s) Hsi-Han Yeh		8. CONTRACT OR GRANT NUMBER(s) AFOSR-82-0207
9. PERFORMING ORGANIZATION NAME AND ADDRESS Department of Electrical Engineering University of Kentucky Lexington KY 40506		10. PROGRAM ELEMENT, PROJECT, TASK AREA & WORK UNIT NUMBERS PE61102F; 2304/D9
11. CONTROLLING OFFICE NAME AND ADDRESS Mathematical & Information Sciences Directorate Air Force Office of Scientific Research Bolling AFB DC 20332		12. REPORT DATE JAN 83 13. NUMBER OF PAGES 80
14. MONITORING AGENCY NAME & ADDRESS(if different from Controlling Office)		15. SECURITY CLASS. (of this report) UNCLASSIFIED 15a. DECLASSIFICATION/DOWNGRADING SCHEDULE

16. DISTRIBUTION STATEMENT (of this Report)
Approved for public release; distribution unlimited.

17. DISTRIBUTION STATEMENT (of the abstract entered in Block 20, if different from Report)

18. SUPPLEMENTARY NOTES

19. KEY WORDS (Continue on reverse side if necessary and identify by block number)
Digitalization; Discrete Maximum Principle; Frequency Response Matching; Discretization; Z-transform; Optimization; Tustin transformation; State-Trajectory Matching; Digital Control System; Model following; Extended Maximum Principle; Z-transfer function; Least-Square fit; Minimum-Integral-Square error; Digital Controller Synthesis.

20. ABSTRACT (Continue on reverse side if necessary and identify by block number)
In converting a continuous-data (analog) controller into a digital controller or in synthesizing a digital controller to have the digital controlled system follow an ideal system, ad hoc approaches such as bilinear or Tustin transform techniques have typically been used. These methods have the advantages of being straight forward and easy to use, and they are intuitively appealing. But the performance of a system digitalized by these approaches resembles the performance of the continuous model only when the sampling period is relatively high, because the dynamics of the plant and the feedback structure of (CONTINUED)

DD FORM 1 JAN 73 1473 EDITION OF 1 NOV 65 IS OBSOLETE

UNCLASSIFIED

SECURITY CLASSIFICATION OF THIS PAGE (When Data Entered)

ITEM #20, CONTINUED: the system are not taken into consideration.

In this study, an attempt is made to match the continuous state trajectory of the digital control with that of its continuout model. Matching the state trajectories instead of the output response assures that the performances of the internal variables of the plant, as well as the output variable, are preserved in the digitalization. The state trajectory matching is quantified by a minimum integral-squared error. The choice of this performance index is motivated by the fact that if the state trajectories of two linear dynamical systems match, the frequency responses of the two systems will also match, as seen by Laplace transforming the state equations.

The mathematical tool used in this research is an extended maximum principle of Pontryagin type, which enables one to synthesize a "staircase" type of optimal control signals, such as the output of a zero-order hold associated with a digital controller. The result is an equivalent discrete-time performance index. Computational verification and performance evaluations and comparisons are made through examples. Computational difficulties special to this method are discussed.

FOREWORD

The research described in this report was the continuation of an effort initiated in the 1981 Summer Faculty Research Program sponsored by the Air Force Office of Scientific Research through the Southeastern Center for Electrical Engineering Education. The 1981 summer research was performed at the Flight Dynamics Laboratory, Wright-Patterson Air Force Base, with the assistance of the Control Analysis Group headed by David K. Bowser. This work was performed in the Department of Electrical Engineering, University of Kentucky, under Air Force Grant AFOSR-82-0207. This report covers work performed from June 1, 1982 to August 31, 1982, plus 20 percent effort for the period from May 1, 1982 to May 15, 1982.

The author wishes to express his appreciation to Mr. David Steele, graduate student in the Department of Electrical Engineering, University of Kentucky, for his assistances in programming the numerical examples and in carrying out the computer simulation. The original version of the computer program that calculates the parameters of the optimal digital controller was written by Dr. Kyung-Sam Choi, Associate Professor of Electrical Engineering, Hong-ik University, Republic of Korea, when he was visiting the University of Kentucky in the academic year 1980-1981.

The author would also like to thank Ms. Cindy Taulbee and Ms. Gail McAlister and the publication staff of the College of Engineering and the University of Kentucky Research Foundation for their efforts in preparing this report.

TABLE OF CONTENTS

LIST OF FIGURES

SECTION I

INTRODUCTION

The digitalization of flight control systems has been of increasing interest to the Air Force. One of the problems confronting the designer is the real-time implementation of advanced control algorithms within the computational capability of the on-board computer. Although digital computer technology continues to advance significantly, new and expanded software requirements for such functions as navigation, display and control manage to keep pace with improvements in computational capability. As a rule, only a small fraction of the CPU frame time is allocated for control law computation. Hence, from the standpoint of implementation, the sampling rate should be sufficiently low in order to allow time for computation and for the computer to be time-shared. But lower limits of the sampling rate are determined by factors such as excessive ratcheting and jittering in the time response, errors due to measurement noise and sensitivity to plant parameter uncertainty and disturbances. The control system designer is then faced with the task of optimizing the performance of the digital control system at a given rate of sampling.

In converting a continuous-data (analog) controller into a digital controller, ad hoc approaches such as bilinear transform and prewarped Tustin transform techniques have typically been used. These methods have the advantage of being straightforward and easy to use, and they are intuitively appealing. But the performance of a system digitalized by these approaches resembles the performance of the baseline (continuous) system only when the sampling frequency is relatively high, because the dynamics of the plant and the feedback structure of the system are not taken into consideration.

Four years ago Rattan and the author of this report presented a method [1] using a complex-curve fitting technique to synthesize the digital controller so that the frequency response of the digitalized system matches that of the original continuous model with a least-square fit. This method was recently applied to a mathematical model of the

longitudinal flight control of the YF-16 fighter aircraft at an altitude of 30,000 ft. and Mach 0.6. Results [2] better than that of Tustin transform approach have been obtained, especially for lower sampling frequencies. However, this method does not take the time-domain performances into consideration; and only the magnitude plots of the frequency responses are matched, without regard to the phase plot. Moreover, the comparison between the frequency response of a continuous system and the frequency response of a digital control system becomes meaningless (see Appendix D) as the signal frequency approaches the folding frequency (one half of the sampling frequency). To compensate for these shortcomings, the state-variable design techniques in the time-domain should be developed.

In a previous study, the author and his associate showed that [3] by using z-transformation technique, a digital controller can always be synthesized so that the output of the digitalized system matches the output of the continuous model at all sampling instants, under the stimulation of the same input.

In this study, an attempt is made to match the continuous state trajectory of the digital control system with that of its analog (continuous-data) model. Matching the state trajectories instead of the output responses assures that the performances of the internal variables of the plant, as well as the output variable, are preserved in the digitalization. It should also be emphasized that the matching is specified over the entire continuous time axis, not just at discrete sampling instants, and is quantified by a minimum integral squared error. The choice of this performance criterion is motivated by the fact that if the state trajectories of two linear dynamical systems match, then frequency responses of the two systems will also match, as seen by Laplace-transforming the state equations.

The mathematical tool used in this research is an extended maximum principle of the Pontryagin type, which enables one to synthesize a "staircase" type of optimal control signals, such as the output signal of a zero-order hold associated with a digital controller. The extended maximum principle was initiated by Chang [4] and further developed by

the author and his co-workers [5-9]. Though not widely used in the technical literature, it is a very effective tool for obtaining the discrete time optimal control policy for an integral performance index, with a minimum amount of mathematical manipulations. It is shown in the sequel (Section VI) that the same result can be derived from the discrete maximum principle and an equivalent discrete-time performance index but through a far more cumbersome procedure.

This research is a continuation of the effort initiated in the 1981 Summer Faculty Research Program sponsored by the Air Force Office of Scientific Research through the Southeastern Center for Electrical Engineering Education, under contract F49620-79-C-0038. In order for this report to be self contained, the mathematical formulation of the problem will be repeated (Section II). The optimal strategy and the digital controller are rederived for the general case (Sections III, IV). Computational verification and performance evaluations and comparisons are presented in Section V, where computational difficulties that are special to this method are discussed. Conclusions and recommendations are given in Section VII.

SECTION II

FORMULATION OF THE DESIGN PROBLEM

Consider a continuous output tracking system (Fig. 1) that has satisfactory (or ideal) performances. The state and output equations of the plant are given by

$$\dot{\underline{x}}_a(t) = A\underline{x}_a(t) + \underline{b}u_m(t) \tag{1}$$

$$y_m(t) = \bar{c}\underline{x}_a(t) + du_m(t) \tag{2}$$

The state and output equations of the controller are given by

$$\dot{\underline{x}}_c(t) = A_c\underline{x}_c(t) + \underline{b}_c e_m(t) \tag{3}$$

$$u_m(t) = \bar{c}_c\underline{x}_c(t) + d_c e_m(t) \tag{4}$$

where $\underline{x}_a(t)$ and $\underline{x}_c(t)$ are n and n_c dimensional vectors, respectively, and $u_m(t)$, $e_m(t)$, $y_m(t)$ and $r(t)$ are scalar functions. The dimensions of the coefficient matrices are commensurate with the vectors with which they associate. The design objective is to replace the controller $G_c(s)$ by a digital controller $D(z)$ such that the state trajectory of the digitalized system matches that of the continuous model as closely as possible. The digital control system is represented by Fig. 2, where $G(s)$ is the same plant as in the continuous model, and $D(z)$ is to be synthesized in such a way that when $r(t)$ is a unit-step function, the performance index

$$J = \frac{1}{2}\int_0^\infty \{[\underline{x}(t) - \underline{x}_a(t)]'Q[\underline{x}(t) - \underline{x}_a(t)] + \beta[u(t) - u_m(t)]^2\}\, dt \tag{5}$$

attains its minimum, where

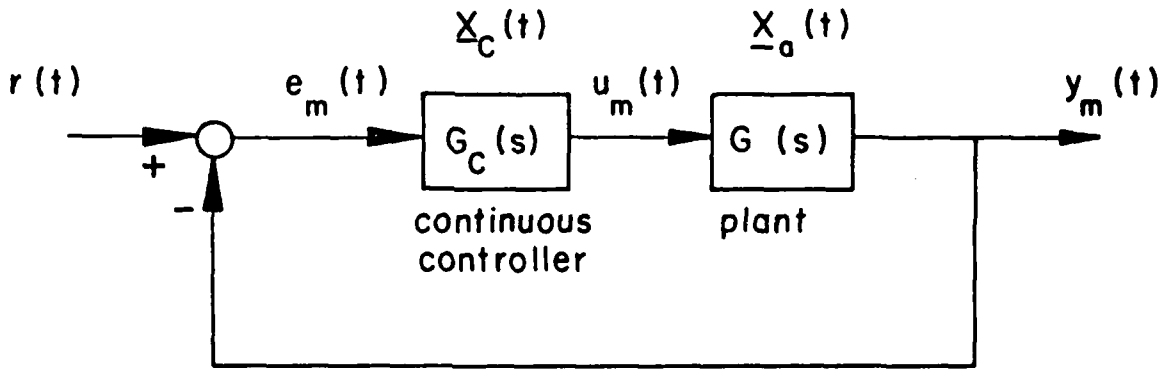

Fig. 1 Continuous System Model

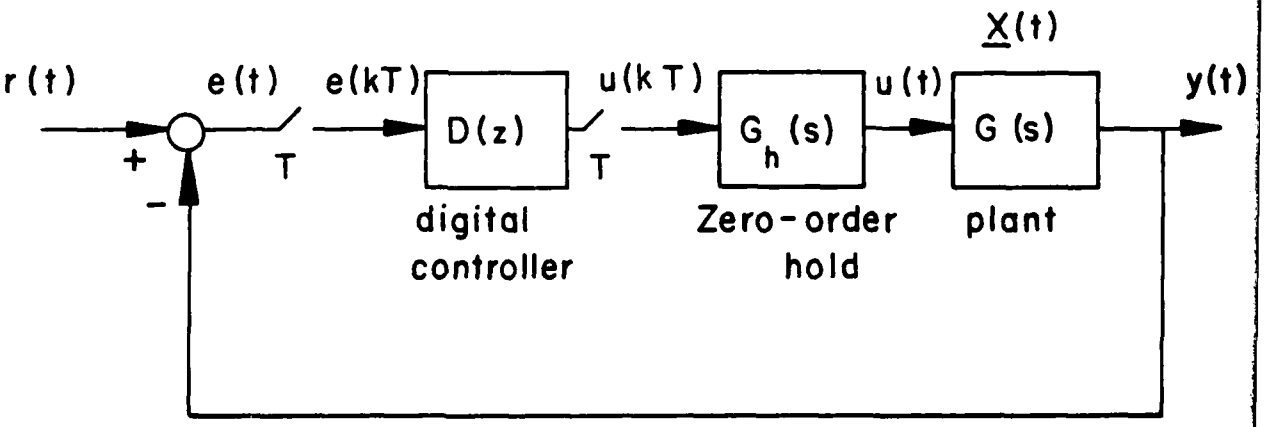

Fig. 2 The Digitalized System

$$Q = \begin{bmatrix} q_1 & 0 & \cdots & 0 \\ 0 & q_2 & \cdots & 0 \\ \vdots & \vdots & & \vdots \\ 0 & 0 & \cdots & q_n \end{bmatrix} ; \quad q_i > 0 , \quad i = 1,2,\cdots,n ; \quad \beta \geq 0 \qquad (6)$$

Note that the performance index is an integral, not a discrete sum. Therefore an attempt is made to match the trajectories over the continuous time axis, not just at the sampling instants. The state and output equations of the plant in the digital control system are

$$\dot{\underline{x}}(t) = A\underline{x}(t) + \underline{b}u(kT) \qquad (7)$$

$$y(t) = \bar{c}\underline{x}(t) + du(kT) \qquad (8)$$

for $kT < t \leq (k + 1)T$, on account of the zero-order hold used in the digital control system (Fig. 2).

SECTION III

THE OPTIMAL CONTROL SEQUENCE

(A) The Extended Maximum Principle

An extended version of the maximum principle of Pontryagin will be used to find the optimal control sequence u(kT), k = 0,1,2,•••, which minimizes the performance index (5). The error sequence e(kT) can be expressed in terms of u(kT), and the digital controller D(z) can be determined by

$$D(z) = \frac{U(z)}{E(z)} \tag{9}$$

where U(z) is the z-transform of u(kT) and E(z) is the z-transform of e(kT).

The original Pontryagin's Maximum Principle cannot be applied to this problem in which the control function must be sampled and held, i.e.,

$$u(t) = u(kT) , \quad kT < t \leq (k+1)T \tag{10}$$

The derivation of Pontryagin's maximum principle is based on the assumption that piece-by-piece patchwork of admissible control functions is again admissible. This condition is not satisfied by the output of a zero-order hold following a constant rate sampler, if the point of patching is selected at an instant other than the sampling instants. However, the extended maximum principle may be applied to the case where the control inputs are outputs of zero-order holds [5-9]. The following derivation follows from Reference [7]. The Hamiltonian function H is formed from the adjoint vector $\underline{p}(t)$, the state derivative $\dot{\underline{x}}(t)$ and the integrand of the performance index as

$$H(\underline{x}(t),\underline{p}(t),u(t)) = \underline{p}'(t)\dot{\underline{x}}(t) - \frac{1}{2}\{[\underline{x}(t) - \underline{x}_a(t)]'Q[\underline{x}(t) - \underline{x}_a(t)] + \beta[u(t) - u_m(t)]^2\} \tag{11}$$

where the prime denotes transpose. Substituting (7) into (11) gives

$$H(\underline{x}(t),\underline{p}(t),u(t)) = p'(t)A\underline{x}(t) + \underline{p}'\underline{b}u(t)$$

$$- \frac{1}{2}\{[\underline{x}(t) - \underline{x}_a(t)]'Q[\underline{x}(t) - \underline{x}_a(t)] + \beta[u(t) - u_m(t)]^2\} \quad (12)$$

The adjoint vector $\underline{p}(t)$ is given by

$$\dot{\underline{p}}(t) = - \frac{\partial}{\partial \underline{x}(t)} H(\underline{x}(t),\underline{p}(t),u(t)) \quad (13)$$

Substituting (12) into (13) gives the adjoint system

$$\dot{\underline{p}}(t) = -A'\underline{p}(t) + Q[\underline{x}(t) - \underline{x}_a(t)] \quad (14)$$

The necessary condition for the control and trajectory to be optimum is that the first variation of the integral of the Hamiltonian is zero, i.e.,

$$\lim_{\varepsilon \to 0} \frac{1}{\varepsilon} \int_0^\infty [H(\underline{x},\underline{p},u + \delta_\varepsilon u) - H(\underline{x},\underline{p},u)]\, dt = 0 \quad (15)$$

where the variable t in the Hamiltonian has been suppressed, and

$$\delta_\varepsilon u(t) = \varepsilon \Delta u(kT) , \quad kT \le t < (k+1)T \quad (16)$$

where $\Delta u(kT)$ is an arbitrary finite variation of $u(kT)$. Substituting (12) and (16) into (15) gives

$$\sum_{k=0}^{\infty} \int_{kT}^{(k+1)T} [\underline{p}'\underline{b} - \beta(u(kT) - u_m(t))]\Delta u(kT)\, dt = 0 \quad (17)$$

Since $\Delta u(kT)$ is an arbitrary constant which may be set independently for each k, (17) implies

$$\int_{kT}^{(k+1)T} [\underline{p}'\underline{b} - \beta(u(kT) - u_m(t))]\, dt = 0 \qquad (18)$$

From (18) the optimal control u(kT) is found to be

$$u(kT) = \frac{1}{\beta T} \int_{kT}^{(k+1)T} [\underline{p}'\underline{b} + \beta u_m(t)]\, dt \qquad (19)$$

The difficulty in the application of the maximum principle is the two-point boundary value problem. In this formulation, the two-point boundary value problem is as follows: For any i, if $x_i(0)$ is given, then $p_i(0)$ is unspecified (remains to be determined from (7), (19) and (14)). If $x_i(0)$ is unspecified (remains to be determined by the maximum principle), then $p_i(0) = 0$. The same rule applies to $x_i(\infty)$ and $p_i(\infty)$.

(B) Determination of the Optimal Control Sequence

In order to compute the optimal control sequence u(kT) from (19), the solution $\underline{p}(t)$ of (14) and an explicit expression of $u_m(t)$ must be found first.

Let the augmented state vector of the model be

$$\underline{x}_m(t) = \begin{bmatrix} \underline{x}_a(t) \\ \underline{x}_c(t) \end{bmatrix} \qquad (20)$$

It follows from Appendix A that

$$\dot{\underline{x}}_m(t) = A_m \underline{x}_m(t) + \underline{b}_m r(t) \qquad (21)$$

$$u_m(t) = \bar{c}_m \underline{x}_m(t) + d_m r(t) \qquad (22)$$

where

$$A_m = \begin{bmatrix} A - \frac{\underline{b}d_c\bar{c}}{1+dd_c} & \frac{\underline{b}\bar{c}_c}{1+dd_c} \\ \frac{-\underline{b}_c\bar{c}}{1+dd_c} & A_c - \frac{\underline{b}_c d\bar{c}_c}{1+dd_c} \end{bmatrix} \tag{23}$$

$$\underline{b}_m = \begin{bmatrix} \frac{\underline{b}d_c}{1+dd_c} \\ \frac{\underline{b}_c}{1+dd_c} \end{bmatrix} \tag{24}$$

$$\bar{c}_m = \begin{bmatrix} \frac{-d_c\bar{c}}{1+dd_c} & \frac{\bar{c}_c}{1+dd_c} \end{bmatrix} \tag{25}$$

and

$$d_m = \frac{d_c}{1+dd_c} \tag{26}$$

Define Q_m to be the $n \times (n+n_c)$ matrix obtained by augmenting n_c columns of zeros to Q, i.e.,

$$Q_m = [Q \quad 0] \tag{27}$$

Then by definition

$$Q\underline{x}_a(t) = Q_m\underline{x}_m(t) \tag{28}$$

Assume that r(t) is a step function, i.e.,

$$r(t) = \begin{cases} \alpha & t \geq 0 \\ 0 & t < 0 \end{cases} \tag{29}$$

It is shown in Appendix B that, for $kT < t \leq (k+1)T$,

$$\underline{x}(t) = \Phi(t-kT)\underline{x}(kT) + \Phi^{s}(t-kT)\underline{b}u(kT) \tag{30}$$

$$\underline{x}_m(t) = \Phi_m(t-kT)\underline{x}_m(kT) + \Phi_m^{s}(t-kT)\underline{b}_m\alpha \tag{31}$$

and

$$\underline{p}(t) = \Psi(t-kT)\underline{p}(kT) + F(t-kT)\underline{x}(kT) + F^{s}(t-kT)\underline{b}u(kT)$$

$$- F_m(t-kT)\underline{x}_m(kT) - F_m^{s}(t-kT)\underline{b}_m\alpha \tag{32}$$

where

$$\Phi(t) = \varepsilon^{At} \tag{33}$$

$$\Phi^{s}(t) = \int_0^t \Phi(\tau)\, d\tau \tag{34}$$

$$\Phi_m(t) = \varepsilon^{A_m t} . \tag{35}$$

$$\Phi_m^{s}(t) = \int_0^t \Phi_m(\tau)\, d\tau \tag{36}$$

$$\Psi(t) = \varepsilon^{-A't} \tag{37}$$

$$F(t) = \int_0^t \Psi(t-\tau)Q\Phi(\tau)\, d\tau = \Psi(t) * Q\Phi(t) \tag{38}$$

$$F^{s}(t) = \int_0^t F(\tau)\, d\tau \tag{39}$$

$$F_m(t) = \int_0^t \Psi(t-\tau)Q_m\Phi_m(\tau)\, d\tau = \Psi(t) * Q_m\Phi_m(t) \tag{40}$$

$$F_m^{s}(t) = \int_0^t F_m(\tau)\, d\tau \tag{41}$$

Substituting (31) and (32) into (19) and solving for u(kT) yields

$$u(kT) = \frac{1}{\beta T - \underline{b}'F^{ss}(T)\underline{b}} \left\{ \underline{b}'\Psi^{s}(T)\underline{p}(kT) + \underline{b}'F^{s}(T)\underline{x}(kT) \right.$$

$$+ [\beta \bar{c}_m \phi_m^{s}(T) - \underline{b}'F_m^{s}(T)]\underline{x}_m(kT)$$

$$\left. + [\beta \bar{c}_m \phi_m^{ss}(T)\underline{b}_m + \beta T d_m - \underline{b}'F_m^{ss}(T)\underline{b}_m]\alpha \right\} \qquad (42)$$

where

$$\Psi^{s}(T) = \int_0^T \Psi(t)\, dt \qquad (43)$$

$$F^{ss}(T) = \int_0^T F^{s}(t)\, dt \qquad (44)$$

$$F_m^{ss}(T) = \int_0^T F_m^{s}(t)\, dt \qquad (45)$$

and

$$\phi_m^{ss}(T) = \int_0^T \phi_m^{s}(t)\, dt \qquad (46)$$

Equation (42) may be used to compute u(kT) iteratively after the two-point boundary problem is solved. In this research, (9) is used to synthesize the digital controller transfer function D(z). The two-point boundary problem still arises and will be treated in the next section.

SECTION IV

THE DIGITAL CONTROLLER

(A) z-Transform of the Optimal Control Sequence

In order to determine U(z) for use in Eq. (9), $\underline{P}(z)$, $\underline{X}(z)$ and $\underline{X}_m(z)$ must be determined first. Setting t = (k + 1)T in (30) - (32) gives

$$\underline{x}[(k+1)T] = \Phi(T)\underline{x}(kT) + \Phi^s(T)\underline{b}u(kT) \tag{47}$$

$$\underline{x}_m[(k+1)T] = \Phi_m(T)\underline{x}_m(kT) + \Phi_m^s(T)\underline{b}_m\alpha \tag{48}$$

$$\underline{p}[(k+1)T] = \Psi(T)\underline{p}(kT) + F(T)\underline{x}(kT) - F_m(T)\underline{x}_m(kT) + F^s(T)\underline{b}u(kT) - F_m^s(T)\underline{b}_m\alpha \tag{49}$$

Taking z-transformation of (47) - (49) gives, respectively,

$$\underline{X}(z) = \hat{\Phi}(z)[z\underline{x}(0) + \Phi^s(T)\underline{b}U(z)] \tag{50}$$

$$\underline{X}_m(z) = \hat{\Phi}_m(z)\left[z\underline{x}_m(0) + \Phi_m^s(T)\underline{b}_m\frac{\alpha z}{z-1}\right] \tag{51}$$

$$\underline{P}(z) = \hat{\Psi}(z)\left[z\underline{p}(0) + F(T)\underline{X}(z) - F_m(T)\underline{X}_m(z) + F^s(T)\underline{b}U(z) - F_m^s(T)\underline{b}_m\frac{\alpha z}{z-1}\right] \tag{52}$$

where

$$\hat{\Phi}(z) = [zI - \Phi(T)]^{-1} \tag{53}$$

$$\hat{\Phi}_m(z) = [zI - \Phi_m(T)]^{-1} \tag{54}$$

$$\hat{\Psi}(z) = [zI - \Psi(T)]^{-1} \tag{55}$$

Substituting (50) and (51) into Eq. (52) gives

$$\underline{P}(z) = \hat{\Psi}(z)\{z\underline{p}(0) + F(T)\hat{\Phi}(z)z\underline{x}(0) - F_m(T)\hat{\Phi}_m(z)z\underline{x}_m(0)$$

$$- [F_m(T)\hat{\Phi}_m(z)\Phi_m^s(T) + F_m^s(T)]\underline{b}_m \frac{\alpha z}{z-1}$$

$$+ [F(T)\hat{\Phi}(z)\Phi^s(T) + F^s(T)]\underline{b}U(z)\} \tag{56}$$

Substituting (50), (51) and (56) into the z-transform of (42), and solving for U(z) yields

$$U(z) = \frac{1}{\beta T - \underline{b}'H(z)\underline{b}}\{\underline{b}'K(z)z\underline{x}(0) + \underline{b}'K_0(z)z\underline{p}(0)$$

$$+ [\beta\bar{c}_m\Phi_m^s(T)\hat{\Phi}_m(z) - \underline{b}'K_m(z)]z\underline{x}_m(0)$$

$$+ [\beta\bar{c}_m(\Phi_m^s(T)\hat{\Phi}_m(z)\Phi_m^s(T) + \Phi_m^{ss}(T))\underline{b}_m - \underline{b}'H_m(z)\underline{b}_m + \beta T d_m]\frac{\alpha z}{z-1}\} \tag{57}$$

where

$$K_m(z) = [\Psi^s(T)\hat{\Psi}(z)F_m(T) + F_m^s(T)]\hat{\Phi}_m(z) \tag{58}$$

$$K(z) = [\Psi^s(T)\hat{\Psi}(z)F(T) + F^s(T)]\hat{\Phi}(z) \tag{59}$$

$$K_0(z) = \Psi^s(T)\hat{\Psi}(z) \tag{60}$$

$$H_m(z) = F_m^{ss}(T) + K_0(z)F_m^s(T) + K_m(z)\Phi_m^s(T) \tag{61}$$

$$H(z) = F^{ss}(T) + K_0(z)F^s(T) + K(z)\Phi^s(T) \tag{62}$$

(B) <u>z-Transform of the Error Sequence</u>

From the block diagram of Fig. 2 and Eqs. (8) and (30) we may write

$$e(t) = r(t) - y(t) = \alpha - y(t) \tag{63}$$

$$y(t) = \bar{c}\Phi(t-kT)\underline{x}(kT) + [\bar{c}\Phi^{s}(t-kT)\underline{b} + d]u(kT) \tag{64}$$

for $kT < t \leq (k+1)T$. Therefore

$$e[(k+1)T] = \alpha - \bar{c}\Phi(T)\underline{x}(kT) - [\bar{c}\Phi^{s}(T)\underline{b} + d]u(kT) \tag{65}$$

Taking z-transform of the above equation gives

$$E(z) = e(0^{+}) + \frac{\alpha}{z-1} - \frac{1}{z}\bar{c}\Phi(T)\underline{X}(z) - \frac{1}{z}[\bar{c}\Phi^{s}(T)\underline{b} + d]U(z) \tag{66}$$

where $e(0^{+})$ is found from (63) and (8) as

$$e(0^{+}) = \alpha - \bar{c}\underline{x}(0^{+}) - du(0^{+}) \tag{67}$$

Substituting (67) and (50) into (66) gives

$$E(z) = \frac{\alpha z}{z-1} - du(0^{+}) - \bar{c}[I + \Phi(T)\hat{\Phi}(z)]\underline{x}(0^{+})$$

$$- \frac{1}{z}[\bar{c}(I + \Phi(T)\hat{\Phi}(z))\Phi^{s}(T)\underline{b} + d]U(z) \tag{68}$$

From the definition of $\hat{\Phi}(z)$ given in (53), it follows that

$$I + \Phi(T)\hat{\Phi}(z) = z\hat{\Phi}(z) \tag{69}$$

Moreover, for most control systems the control signal does not supply power to the output. Hence $d = 0$ and $E(z)$ of (68) may be written as

$$E(z) = \frac{\alpha z}{z-1} - \bar{c}z\hat{\Phi}(z)\underline{x}(0^{+}) - \bar{c}\hat{\Phi}(z)\Phi^{s}(T)\underline{b}U(z) \tag{70}$$

By virtue of the relationship given in (9), the z-transfer function of the digital controller may now be written, provided that the initial conditions $\underline{x}(0)$, $\underline{x}_{m}(0)$ and $\underline{p}(0)$ are known.

(c) The z-Transfer Function of the Digital Controller

In the model-following design, the initial state $\underline{x}_m(0)$ of the model may be taken to be zero. But if $\underline{x}(0)$ is given, the $\underline{p}(0)$ cannot be arbitrarily specified. The maximum principle requires that $\underline{p}(0)$ be such that Eqs. (7), (14) and (19) yield an optimal control sequence that drives the system from the given $\underline{x}(0)$ to a prespecified final state $\underline{x}(\infty)$, or results in $\underline{p}(\infty) = 0$ if the final state is unspecified (free). Numerical determination of $\underline{p}(0)$ for given $\underline{x}(\infty)$ or $\underline{p}(\infty)$ is virtually impossible for systems requiring a large number of sampling periods to run, because either matrix A or $-A'$ has eigenvalues in the unstable region. On the other hand, if $\underline{x}(0)$ is unspecified, $\underline{p}(0)$ must be set equal to zero. But then $\underline{x}(0)$ is determined by Eqs. (7), (14) and (19) and the final condition, which is either at a given value of $\underline{x}(\infty)$ or at $\underline{p}(\infty) = 0$. Again, numerical determination of $\underline{x}(0)$ is impractical for systems requiring a large number of sampling periods to run.

For the system under consideration, the state trajectory of the continuous model is assumed to start from $\underline{x}_m(0) = 0$. Let $\underline{x}(0)$, the initial state of the plant of the digital control system, be unspecified. Then $\underline{p}(0) = 0$. However, since the minimization of the performance index given in (5) means the continuous matching of $\underline{x}(t)$ with $\underline{x}_a(t)$ over an infinitely long period of time, it is reasonable to conjecture that $\underline{x}(t)$ starts at the same point as $\underline{x}_a(t)$, or very close to it, provided that the sampling frequency is considerably higher than the natural frequency of the control system. Hence the initial condition may be chosen as

$$\underline{x}_m(0) = 0 \tag{71}$$

$$\underline{x}(0) = 0 \tag{72}$$

$$\underline{p}(0) = 0 \tag{73}$$

Substituting these conditions into Eqs. (57) and (70), and using the resulting expressions in the right-hand side of (9), we obtain

$$\frac{1}{D(z)} = \frac{E(z)}{U(z)} = -\bar{c}\Phi(z)\Phi^{s}(T)\underline{b}$$

$$+ \frac{\beta T - \underline{b}'H(z)\underline{b}}{\beta\bar{c}_m[\phi_m^{s}(T)\hat{\phi}_m(z)\phi_m^{s}(T) + \phi_m^{ss}(T)]\underline{b}_m - \underline{b}'H_m(z)\underline{b}_m + \beta T d_m} \qquad (74)$$

It should also be recognized that

$$\bar{c}\Phi(z)\Phi^{s}(T)\underline{b} + d = \text{z-transform of } \left[\frac{1-\epsilon^{-Ts}}{s} G(s)\right] \qquad (75)$$

For $\beta = 0$, the digital controller is obtained from (74) as

$$D(z) = \frac{1}{\frac{\underline{b}'H(z)\underline{b}'}{\underline{b}'H_m(z)\underline{b}'_m} - \bar{c}\hat{\Phi}(z)\Phi^{s}(T)\underline{b}} \qquad (76)$$

Note that Eq. (19) cannot be used to find u(kT) for $\beta = 0$. But Eq. (18) becomes

$$\int_{kT}^{(k+1)T} \underline{p}'\underline{b}\, dt = 0 \qquad (77)$$

Since $\underline{p}$ depends on u(kT), (77) can be used to derive the optimal control sequence. This approach was taken in the previous project [10] and the digital controller of (76) was obtained.

(D) The Closed-Loop Transfer Function

Let $\overline{G_h G}(z)$ denote the z-transform of $\frac{1-\epsilon^{-Ts}}{s} G(s)$, i.e.,

$$\overline{G_h G}(z) = \bar{c}\hat{\Phi}(z)\Phi^{s}(T)\underline{b} \qquad (78)$$

Let

$$G_m(z) = \frac{\underline{b}'H_m(z)\underline{b}_m}{\underline{b}'H(z)\underline{b}} \qquad (79)$$

The z-transfer function of the closed-loop system of Fig. 2 is given by

$$\frac{Y(z)}{R(z)} = \frac{D(z)\overline{G_h G}(z)}{1 + D(z)\overline{G_h G}(z)} \tag{80}$$

If the digital controller of (76) is used, D(z) may be written as

$$D(z) = \frac{G_m(z)}{1 - G_m(z)\overline{G_h G}(z)} \tag{81}$$

Substituting (81) into (80) yields

$$\frac{Y(z)}{R(z)} = G_m(z)\overline{G_h G}(z) = \frac{\underline{b}'H_m(z)\underline{b}_m}{\underline{b}'H(z)\underline{b}}\,\overline{G_h G}(z) \tag{82}$$

Thus the optimal model-following design of digital controller can be achieved by the Guillemin-Truxal approach [11] which selects a digital controller transfer function algebraically so that the closed-loop z-transfer function is the product of the z-transfer function of the plant with a zero-order hold and a correction factor $G_m(z)$ given by (79).

It is readily observed from (58) - (62) that

(1) Poles of $H_m(z)$ are eigenvalues of $\varepsilon^{-A'T}$ and $\varepsilon^{A_m T}$,

(2) Poles of H(z) are eigenvalues of $\varepsilon^{-A'T}$ and ε^{AT}.

Since the poles of $\overline{G_h G}(z)$ are eigenvalues of ε^{AT}, what the multiplication factor $G_m(z)$ in (82) actually does is, among other things, to replace the poles of $\overline{G_h G}(z)$ by z-plane poles of the continuous model with samplers connected to in input and the output. Thus the closed-loop digitalized system will have poles of the sampled continuous model, which are eigenvalues of $\varepsilon^{A_m T}$.

The stability conditions of the digitalized system is given in [12]. The system is easily stabilized if all diagonal elements of Q are positive. It is also observed from (82) that if the closed-loop system is stable, then any zeros of $\underline{b}'H(z)\underline{b}$ outside the unit circle must be cancelled by

some zeros of $\underline{b}'H_m(z)\underline{b}_m$. Theoretically, zeros of $\underline{b}'H(z)\underline{b}$ outside the unit circle may be cancelled by some zeros of $\overline{G_h G}(z)$ but such a system is not realizable.

(E) Controller In the Feedback Path

When the controller is in the feedback path, as in Fig. 3 and Fig. 4, Formulas (74) and (76) no longer apply and should be rederived. In this case, the system equations (1) - (4) and (7) - (8) are replaced by

$$\begin{cases} \dot{\underline{x}}_a(t) = A\,\underline{x}_a(t) + \underline{b}\,e_m(t) & (83) \\ y_m(t) = \tilde{c}\,\underline{x}_a(t) + d\,e_m(t) & (84) \end{cases}$$

$$\begin{cases} \dot{\underline{x}}_c(t) = A_c\,\underline{x}_c(t) + \underline{b}_c\,y_m(t) & (85) \\ v_m(t) = \bar{c}_c\,\underline{x}_c(t) + d_c\,y_m(t) & (86) \end{cases}$$

and

$$\begin{cases} \dot{\underline{x}}(t) = A\,\underline{x}(t) + \underline{b}\,e(kT) & (87) \\ y(t) = \bar{c}\,x(t) + d\,e(kT) & (88) \end{cases}$$

respectively. The derivation follows a similar pattern as that of (74) and (76), and will not be repeated here. The result for the case of $\beta = 0$ is given as follows:

$$D_1(z) = \frac{V(z)}{Y(z)} = \frac{\left[1 - \dfrac{\underline{b}'H_m(z)\underline{b}_m}{\underline{b}'H(z)\underline{b}}\right]\dfrac{z}{z-1}}{\dfrac{\underline{b}'F_m^{ss}(T)\underline{b}_m}{\underline{b}'F^{ss}(T)\underline{b}}\,d + \left[\bar{c}\,\bar{\Phi}(z)\bar{\Phi}^{s}(T)\underline{b} + \dfrac{d}{z}\right]\dfrac{\underline{b}'H_m(z)\underline{b}_m}{\underline{b}'H(z)\underline{b}} \cdot \dfrac{z}{z-1}} \qquad (89)$$

Again, for $d = 0$,

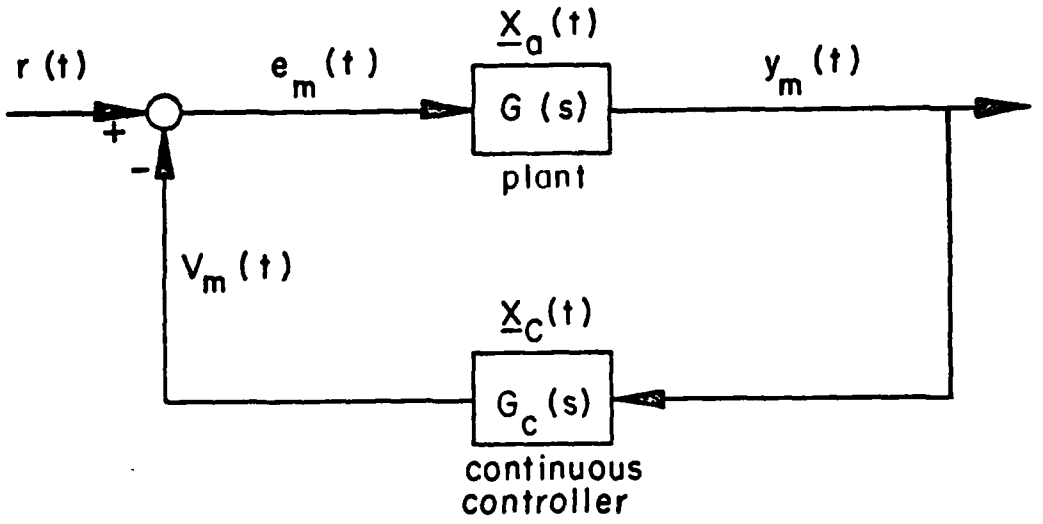

Fig. 3 Continuous System Model

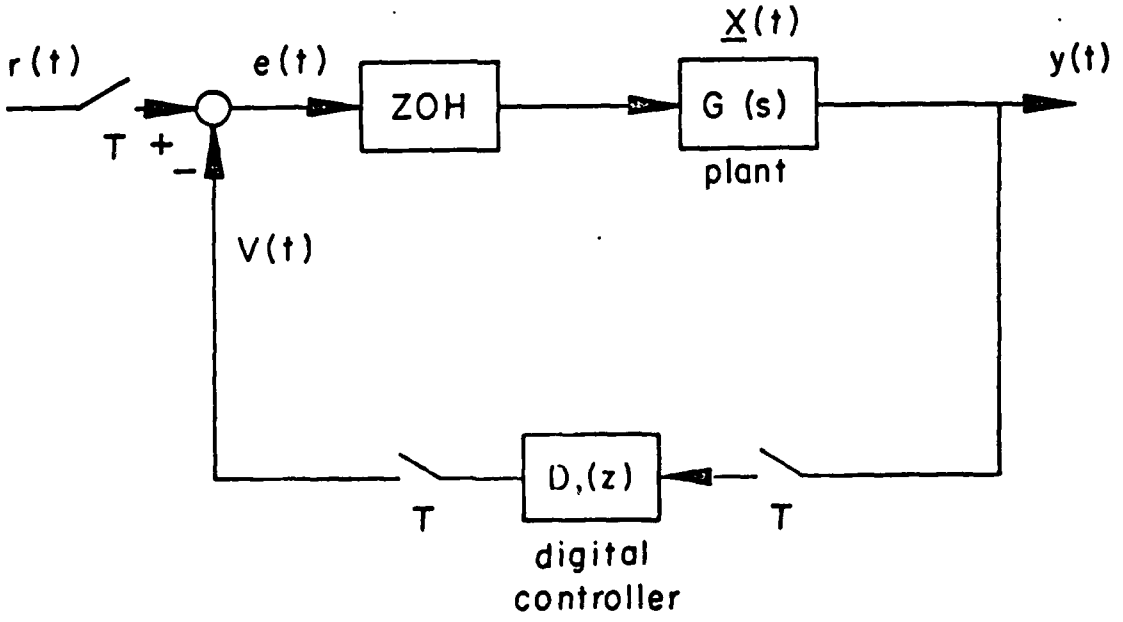

Fig. 4 The Digitalized System

$$D_1(z) = \frac{\underline{b}'[H(z)\underline{b} - H_m(z)\underline{b}_m]}{[\bar{c}\,\Phi(z)\Phi^s(t)\underline{b}][\underline{b}'H_m(z)\underline{b}_m]} \tag{90}$$

where $H(z)$, $H_m(z)$, $\Phi(z)$, and $\Phi^s(T)$ are again given by (62), (61), (53), and (34), respectively, but A_m and $\underline{b}_m$ are now given by:

$$A_m = \begin{bmatrix} A - \dfrac{\underline{b}d_c\bar{c}}{1 + dd_c} & \dfrac{-\underline{b}\bar{c}_c}{1 + dd_c} \\ \dfrac{b_c\bar{c}}{1 + dd_c} & A_c - \dfrac{\underline{b}_c d\bar{c}_c}{1 + dd_c} \end{bmatrix} \tag{91}$$

$$\underline{b}_m = \begin{bmatrix} \dfrac{\underline{b}}{1 + dd_c} \\ \dfrac{b_c d}{1 + dd_c} \end{bmatrix} \tag{92}$$

which are different from their previous definitions of (23) and (24).

It is interesting to see that for the control system of Fig. 4 with a digital controller given by (90), the closed-loop transfer function is again given by (82).

Careful examination of (90), in view of (58) - (62), shows that the digital controller $D_1(z)$ is not realizable, namely, the numerator polynomial of $D_1(z)$ is one degree higher than that of the denominator. To remedy for this, the digitalized system can be implemented as in Fig. 5, which can be derived as follows. First, $V(z)$ of Fig. 4 is found to be

$$V(z) = \left[1 - \frac{\underline{b}'H_m(z)\underline{b}_m}{\underline{b}'H(z)\underline{b}}\right]\frac{\alpha z}{z - 1} \tag{93}$$

In view of (58) - (62), the initial value $v(0)$ is found to be

$$v(0) = \lim_{z\to\infty} V(z) = \left[1 - \frac{\underline{b}'F_m^{ss}(T)\underline{b}_m}{\underline{b}'F^{ss}(T)\underline{b}}\right]\alpha \tag{94}$$

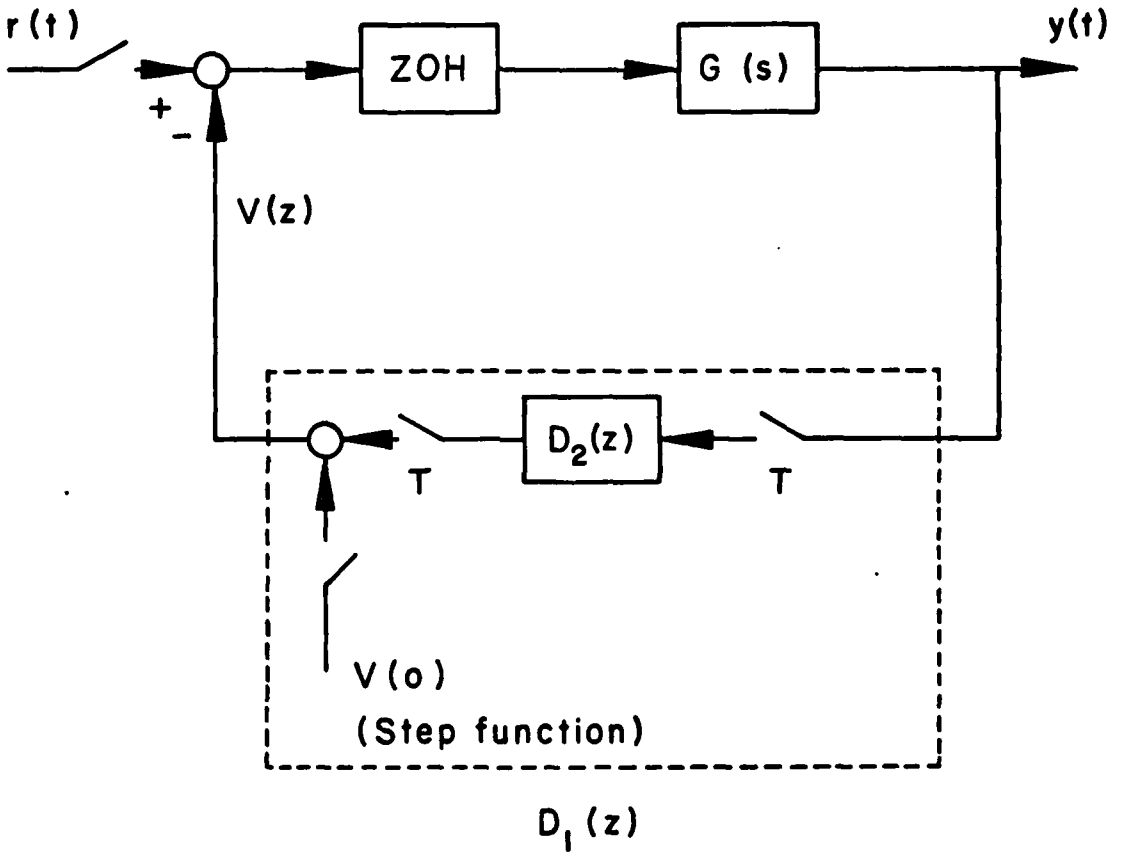

Fig. 5 Realization of The Feedback Digital Controller $D_1(z)$

Thus, when r(t) is a step function of magnitude α,

$$D_2(z) = \frac{V(z) - \frac{v(0)z}{z-1}}{Y(z)}$$

$$= \frac{\frac{\underline{b}'F_m^{ss}(T)\underline{b}_m}{\underline{b}'F(T)\underline{b}} \cdot \frac{\underline{b}'H(z)\underline{b}}{\underline{b}'H_m(z)\underline{b}_m} - 1}{\overline{c\hat{\Phi}}(z)\phi^s(T)\underline{b}} \qquad (95)$$

The digital controller $D_2(z)$ of (95) is realizable, on account of (53) - (55) and (58) - (62).

SECTION V

COMPUTATIONAL VERIFICATION

Attempts have been made to verify the end results through the numerical computations of the transfer functions of the digital controllers and the evaluations of the performances for three examples. For the two lower order systems, excellent time responses of the overall closed-loop digital control systems and satisfactory frequency responses were obtained. The other example was the inner loop of the longitudinal control of YF-16 fighter aircraft at 30,000 ft altitude at Mach 0.6. Limited by the capability of the available computer programs, the result for the last example was unsatisfactory, hence not presented. The computational difficulties and recommendations will be discussed later.

In comparing the frequency responses for the following examples, the expression

$$\frac{Y(\epsilon^{j\omega T})}{R(\epsilon^{j\omega T})} = \left. \frac{D(z)\overline{G_h G}(z)}{1 + D(z)\overline{G_h G}(z)} \right|_{z \to \epsilon^{j\omega T}} \tag{96}$$

is used for the frequency response of a digital control system represented by Fig. 2. It should be noted that, in light of the concept developed in Appendix D, there does not exist a closed-form expression of the frequency response of a digital control system. It is neither represented by (96), nor is it represented by

$$\frac{Y(j\omega)}{R(j\omega)} = \frac{D(\epsilon^{j\omega T}) \dfrac{1 - \epsilon^{-j\omega T}}{j\omega} G(j\omega)}{1 + D(\epsilon^{j\omega T}) G_h G(\epsilon^{j\omega T})} \tag{97}$$

Example 1. The end result given in (74) or (76) is computationally complicated. It will be demonstrated through simple examples first. Referring to Fig. 1 and Fig. 2, let the plant and the controller be

$$G(s) = \frac{1}{s + 1} \tag{98}$$

and

$$G_c(s) = \frac{s + 2}{s} \tag{99}$$

The coefficients in the state variable model are

$$A = [-1] \quad \underline{b} = [1] \quad \overline{c} = [1] \quad d = 0 \tag{100}$$

$$A_c = [0] \quad \underline{b}_c = [1] \quad \overline{c}_c = [2] \quad d_c = 1 \tag{101}$$

We choose $Q = 1$, $Q_m = [1 \quad 0]$ and $\beta = 0$. The sampling period is chosen to be relatively large because the system is a slow one. Otherwise, conversion to digital control would not have been a problem. We shall consider the cases of $T = 0.5$ sec., $T = 1$ sec. and $T = 2$ sec.

Case 1. $T = 0.5$ sec.

Implementation of (76) on the computer program gives

$$D(z) = \frac{1.1017(z - 0.3682)(z + 0.3078)(z - 0.6065)(z + 4.1231)}{(z - 1)(z + 0.2769)(z - 0.5399)(z + 3.8149)} \tag{102}$$

Since the closed-loop system is stable (integral-squared error with respect to a stable model is minimized), the pole and zero of (102) outside the unit circle should not be implemented. Since the performance of the digital control system should match its continuous model only at low frequencies, the controller transfer function of (102) may be approximated by setting $z = 1$ in the factors $(z + 4.1231)$ and $(z + 3.8149)$. Thus

$$D(z) = \frac{1.1722(z - 0.3682)(z + 0.3078)(z - 0.6065)}{(z - 1)(z + 0.2769)(z - 0.5399)} \tag{103}$$

For the purpose of comparison, the controller $G_c(s)$ is discretized by prewarped Tustin transformation (substituting s by $\frac{2}{T}\frac{z - 1}{z + 1}$ and 2 by $\frac{T}{2} \times 2$ respectively, in $G_c(s)$):

$$D_t(z) = \frac{1.5463(z - 0.2934)}{z - 1} \tag{104}$$

If $G_c(s)$ is discretized by impulse invariant transformation, then

$$D_i(z) = \frac{3z - 1}{z - 1} \tag{105}$$

Case 2. T = 1 sec.

Implementing (76) on the computer program gives

$$D(z) = \frac{1.16415(z - 0.3679)(z + 0.3405)(z - 0.1362)(z + 4.3678)}{(z - 1)(z - 0.2384)(z + 0.2978)(z + 4.0066)} \tag{106}$$

Discounting the pole and zero outside the unit circle by setting z = 1 in the corresponding factors gives the stable controller as

$$D(z) = \frac{1.248(z - 0.3679)(z + 0.3405)(z - 0.1362)}{(z - 1)(z - 0.2384)(z + 0.2979)} \tag{107}$$

The prewarped Tustin transformation and impulse invariant transformation of $G_c(s)$ at T = 1 are given by, respectively,

$$D_t(z) = \frac{2.5574(z + 0.218)}{z - 1} \tag{108}$$

$$D_i(z) = \frac{3z - 1}{z - 1} \tag{109}$$

Case 3. T = 2 sec.

$$D(z) = \frac{1.2145944(z - 0.1353)(z + 0.2804)(z - 0.0065)(z + 4.7494)}{(z - 1)(z + 0.2701)(z - 0.0221)(z + 4.6059)} \tag{110}$$

Discounting the unstable pole and zero gives:

$$D(z) = \frac{1.2656(z - 0.1353)(z + 0.2804)(z - 0.0065)}{(z - 1)(z + 0.2701)(z - 0.0221)} \tag{111}$$

The prewarped Tustin transformation and impulse invariant transformation of $G_c(s)$ at T = 2 sec. are, respectively,

$$D_t(z) = \frac{-1.185(z + 2.687)}{(z - 1)} \tag{112}$$

$$D_i(z) = \frac{3z - 1}{z - 1} \tag{113}$$

The comparison of unit-step responses of the closed-loop systems using $D_i(z)$, $D_t(z)$ and $D(z)$ are shown in Fig. 6 and Fig. 7. The comparison for T = 2 is not plotted because the performances of $D_t(z)$ and $D_i(z)$ are too poor. Fig. 8 compares the time responses of the state trajectory matching design at three different sampling frequencies. Closed-loop frequency responses are shown in Figs. 9, 10 and 11.

Example 2. In this example we use a system that was used in Reference [1] in order to compare results with the frequency response matching method for digitalizing the continuous controller. Referring again to Fig. 1, let the plant and the continuous controller be

$$G(s) = \frac{10}{s(s + 1)} \tag{114}$$

and

$$G_c(s) = \frac{1 + \frac{s}{2.4}}{1 + \frac{s}{7.2}} \tag{115}$$

respectively. The coefficients in the state-variable model are:

$$A = \begin{bmatrix} 0 & 1 \\ 0 & -1 \end{bmatrix} \qquad \underline{b} = \begin{bmatrix} 0 \\ 10 \end{bmatrix} \tag{116}$$

$$\bar{c} = [1 \quad 0] \qquad d = [0] \tag{117}$$

$$A_c = [-7.2] \qquad \underline{b}_c = [7.2] \tag{118}$$

$$\bar{C}_c = [-2] \qquad d_c = [3] \tag{119}$$

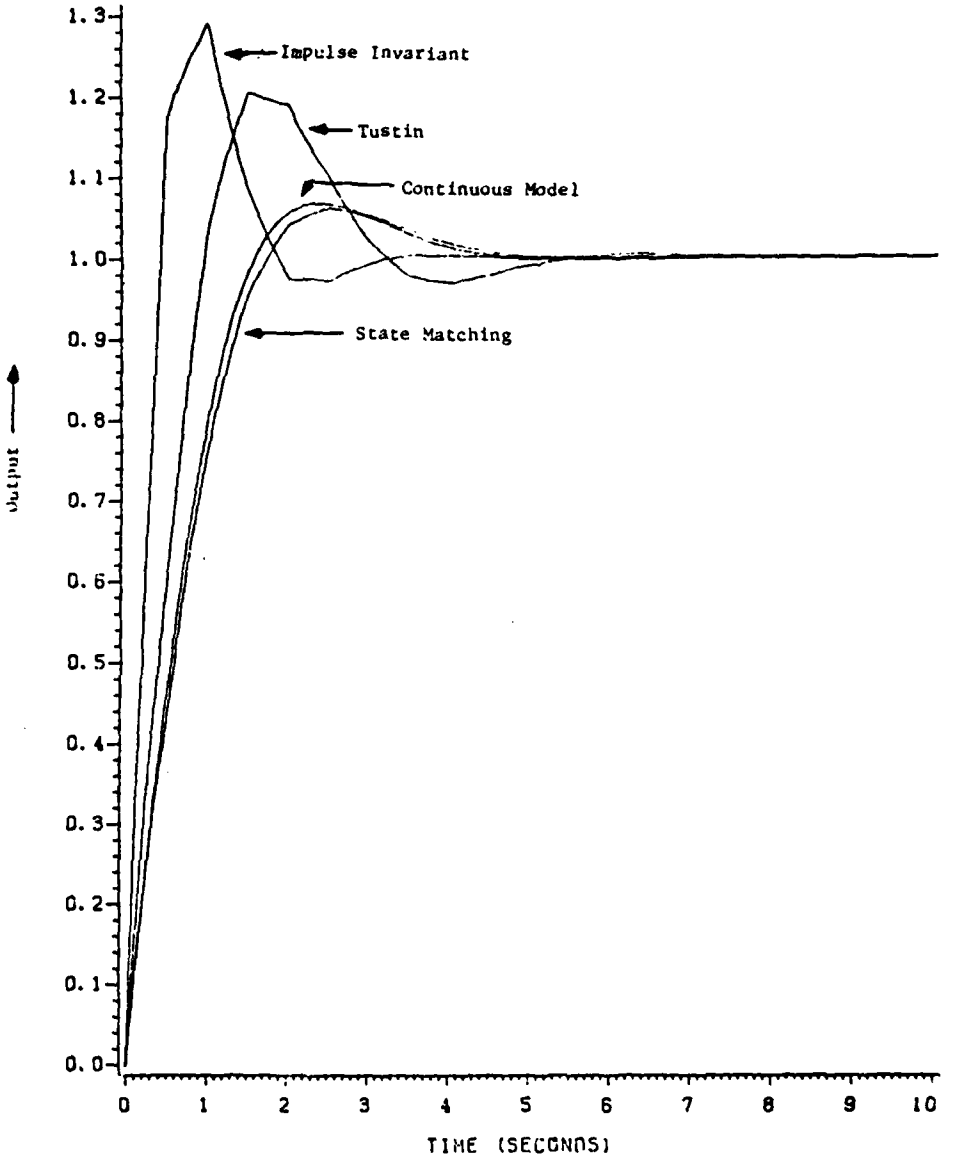

Figure 6. Comparison of Unit-Step Responses of Example 1, T = 0.5.

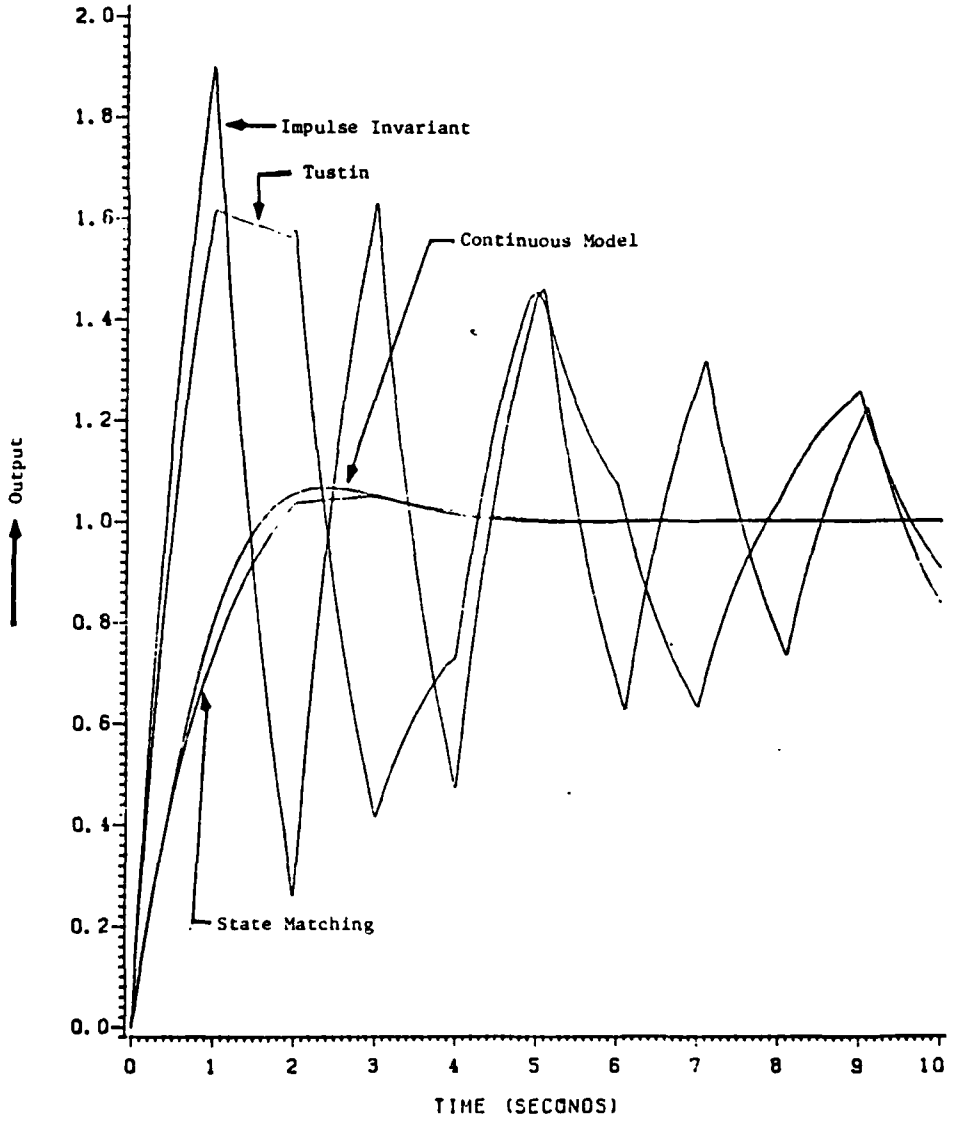

Figure 7. Comparison of Unit-Step Responses of Example 1, T = 1.0

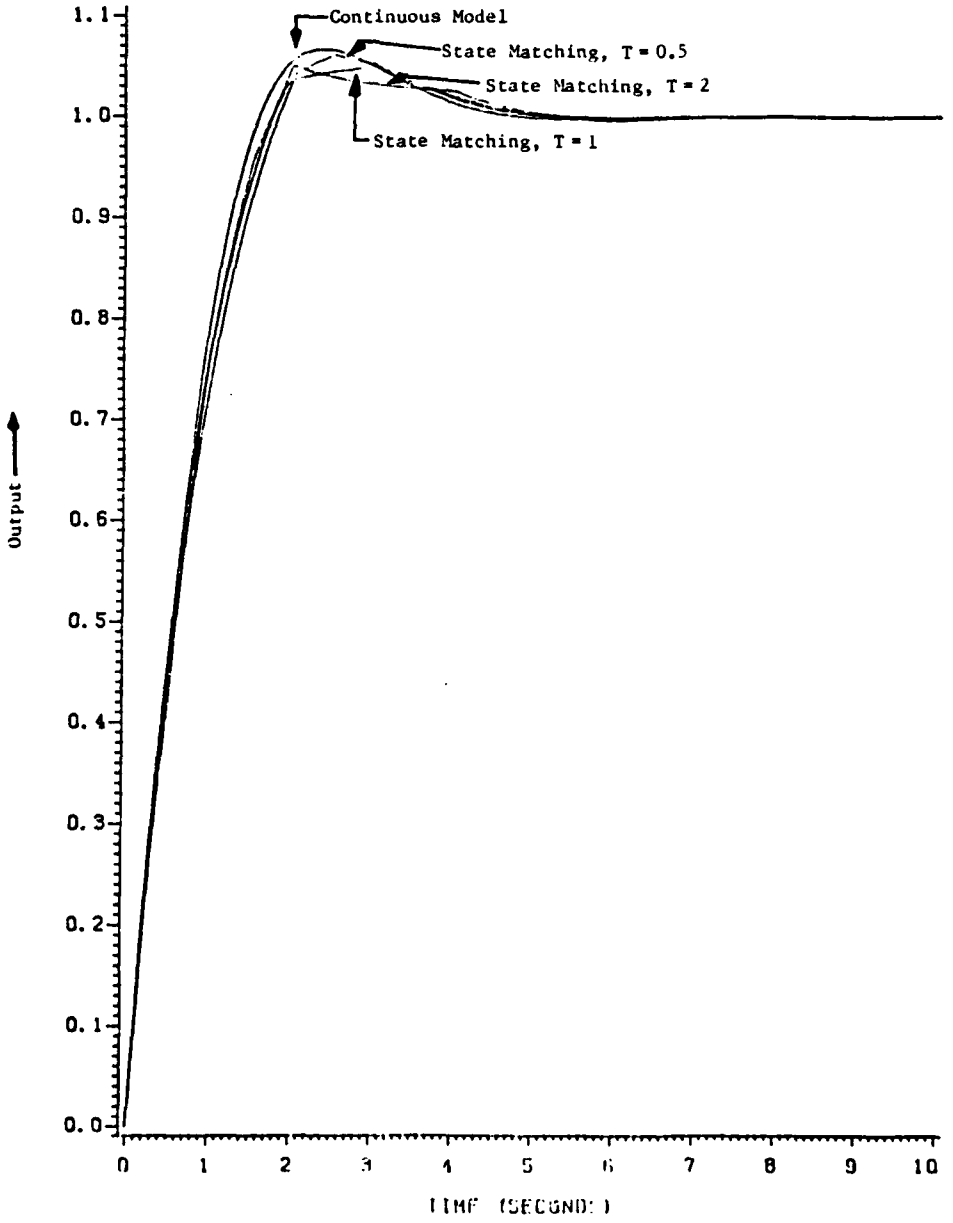

Figure 8. Unit-Step Responses of the State-Trajectory-Matching Design at Different Sampling Frequencies

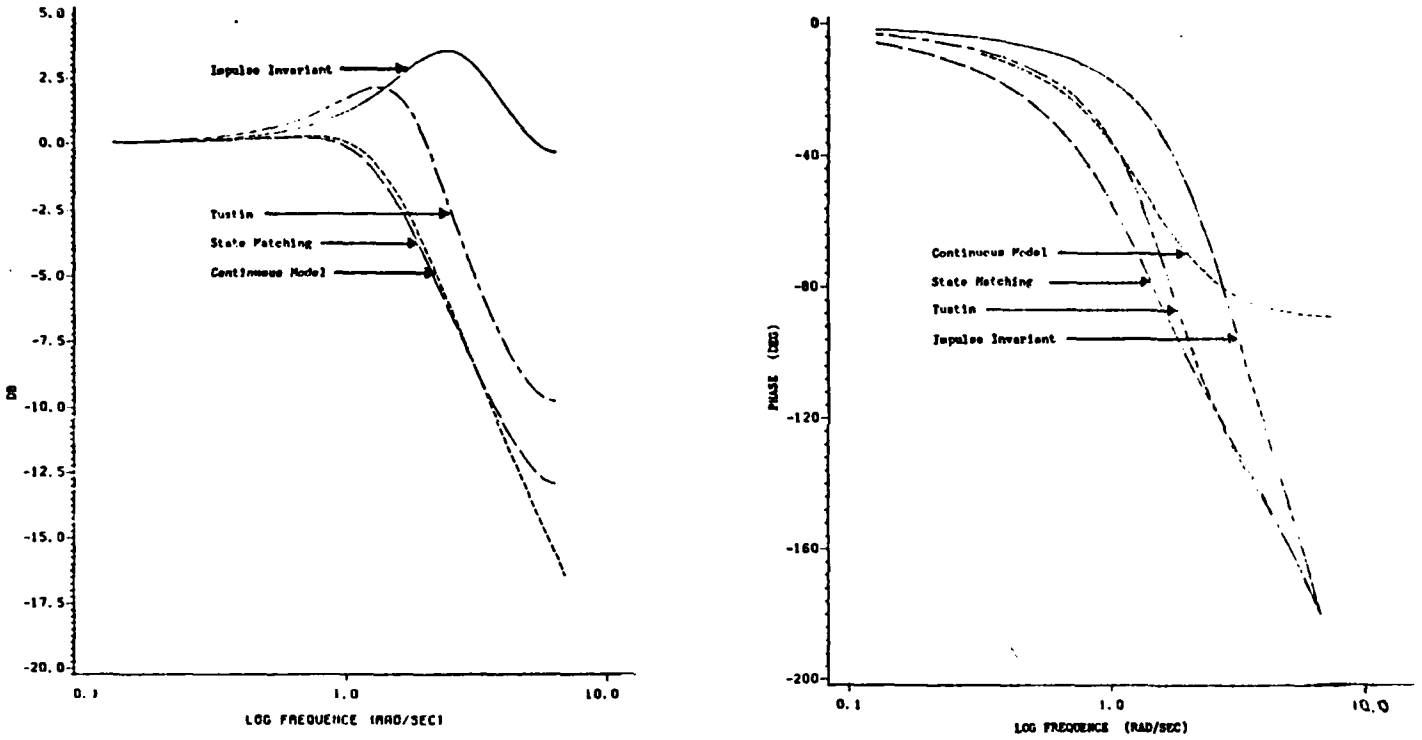

(a) DB vs omega

(b) phase vs omega

Figure 9. Comparison of Closed-loop Frequency Responses of Example 1, T = 0.5

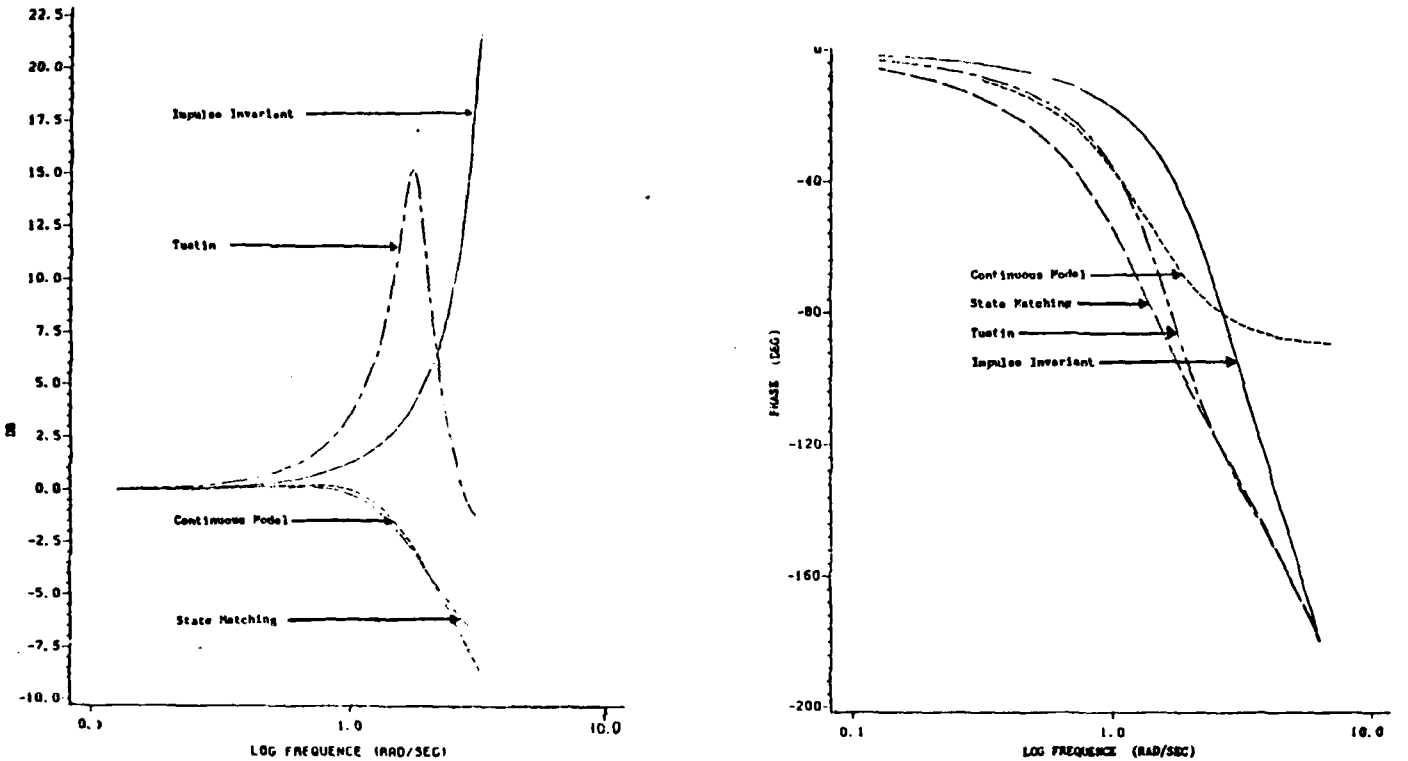

(a) DB vs omega

(b) phase vs omega

Figure 10. Comparison of Closed-loop Frequency Responses of Example 1, T = 1.0

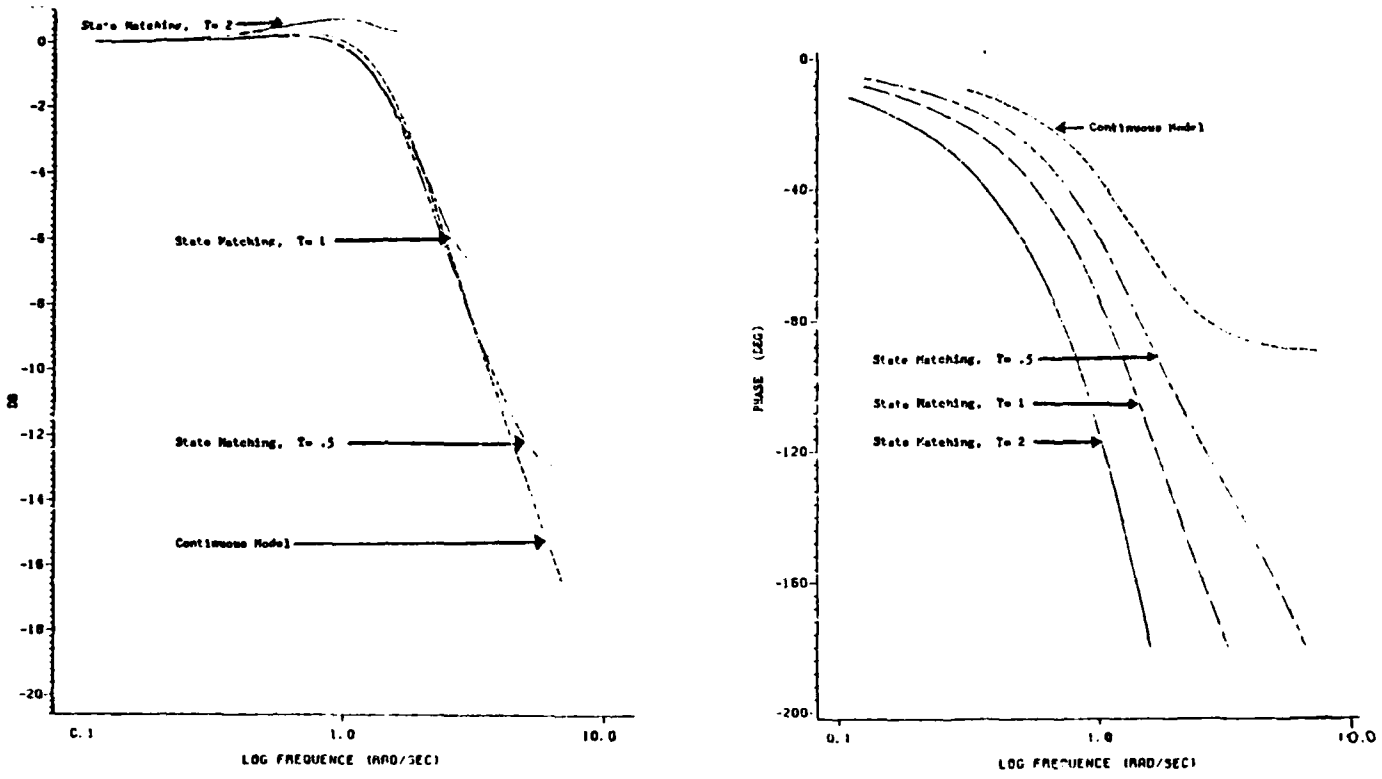

(a) DB vs omega

(b) phase vs omega

Figure 11. Closed-loop Frequency Responses of the State Trajectory Matching Design at Different Sampling Frequencies

We choose

$$A = \begin{bmatrix} 1 & 0 \\ 0 & 1 \end{bmatrix} \qquad Q_m = \begin{bmatrix} 1 & 0 & 0 \\ 0 & 1 & 0 \end{bmatrix} \tag{120}$$

and consider the cases of T = 0.05, T = 0.15 and T = 0.30. Note that for T = 0.3, the sampling frequency is only slightly above twice the bandwidth of the closed-loop system. For this system, digitalization by Tustin transformation gives inferior performances both in the time domain and the frequency domain, and can be found in [15]. Hence, comparison with Tustin method will not be presented. Performance comparisons will be made with the frequency response matching method of Reference [1].

Case 1. T = 0.05

Implementing (76) on the computer program gives

$$D(z) = \frac{2.8219(z - 1)(z - 0.9512)(z + 0.2527)(z - 0.8869)}{(z - 0.9995)(z - 0.9533)(z + 0.2682)(z - 0.9421)}$$

$$\times \frac{(z - 0.9512)(z - 1.0513)(z + 3.5096)}{(z - 0.6742)(z - 1.0514)(z + 3.7310)} \tag{121}$$

Simplifying D(z) by cancelling the poles and zeros that are very close together and discounting the pole and zero outside the unit circle (by setting z = 1 in those factors) gives the reduced version of D(z) as

$$D(z) = \frac{2.6898(z - 0.9512)(z + 0.2527)(z - 0.8869)}{(z - 0.9421)(z + 0.2682)(z - 0.6742)} \tag{122}$$

Note that the zero at 0.9512 in D(z) is also a pole of $\overline{G_h G}(z)$, the z-transform of $\frac{1 - e^{-Ts}}{s} G(s)$.

An attempt has been made to obtain a digital controller via frequency response matching method of Reference [1] for comparison. But the method failed to provide a stable digital control system for T = 0.05.

Case 2. T = 0.15

Implementing (76) on the computer program for T = 0.15 yields

$$D(z) = \frac{2.6577(z + 0.2265)(z - 0.6977)(z - 0.8607)^2}{(z - 0.2040)(z + 0.2771)(z - 0.8607)(z - 0.8090)}$$

$$\times \frac{(z - 1)(z - 1.1618)(z + 3.0744)}{(z - 1)(z - 1.1618)(z + 3.7062)} \tag{123}$$

The reduced model of $D(z)$ is

$$D(z) = \frac{2.294(z + 0.2265)(z - 0.6977)(z - 0.8607)}{(z + 0.2771)(z - 0.2040)(z - 0.8090)} \tag{124}$$

In applying the frequency response matching method, one can specify the order of the digital controller desired. The first and second order digital controller obtained by the frequency response matching method are [1],

$$D_{f1}(z) = \frac{3.6787(z - 0.6275)}{z + 0.3837} \tag{125}$$

and

$$D_{f2}(z) = \frac{3.96 - 3.65z^{-1} + 0.56z^{-2}}{1 + 0.34z^{-1} - 0.384z^{-2}} \tag{126}$$

Results of similation shows that while the frequency domain performance of the second order controller seems to be slightly better than the first order controller, ratcheting and jittering begin to appear in the time response of the system using the second order controller. Hence in order not to overcrowd the graphs, the second order controller is regarded as undesirable and not used in the performance comparison, and higher order controllers by the frequency response matching method are not sought.

Case 3. $T = 0.30$

The transfer function of the digital controller (Eq. (76)) is found to be

$$D(z) = \frac{2.0175(z + 0.1958)(z - 0.4865)(z - 0.7394)}{(z + 0.1099)(z + 0.3678)(z - 0.6012)}$$

$$\times \frac{(z - 0.7423)(z - 1)(z - 1.3499)(z + 2.4504)}{(z - 0.7414)(z - 1)(z - 1.3499)(z + 3.5534)} \qquad (127)$$

The reduced model of D(z) is

$$D(z) = \frac{1.5288(z + 0.1958)(z - 0.4865)(z - 0.7394)}{(z + 0.1099)(z + 0.3678)(z - 0.6012)} \qquad (128)$$

For T = 0.30, the frequency response method fails to produce stable digital controller again.

The unit-step responses at the output of the state trajectory matching design, the continuous model and the system obtained by frequency response matching method (first-order controller only) for T = 0.15 are compared in Fig. 12. Fig. 13 compares the squared errors of the time-responses of the state trajectory matching design with the frequency response matching design using the continuous model as the ideal response. The time responses of the second state variable $\dot{y}$ of the two designs at T = 0.15 are shown in Fig. 14. The squared errors are shown in Fig. 15. Comparisons of time domain performances of the state trajectory matching design for different sampling frequencies are made in Fig. 16 and Fig. 17. The frequency response comparisons are made in Fig. 18 and Fig. 19.

It should be noted that, although a first glance of Fig. 12 may give the impression that the frequency matching method and the state-trajectory matching method both give about the same time-domain performances, Fig. 13 shows that the state-trajectory matching gives a much better design. Fig. 14 and Fig. 15 show that the state matching method yields much better step response in the other state variable too. Although the frequency matching method seems to yield a frequency response that matches the frequency response of the continuous model better at the higher frequency range than that of the state matching design (Fig. 19), Appendix D suggests that the close matching of frequency responses between a discrete time system and a continuous system at the

higher frequency range is not only meaningless, but also undesirable if the discrete time system is actually a digitally controlled continuous system.

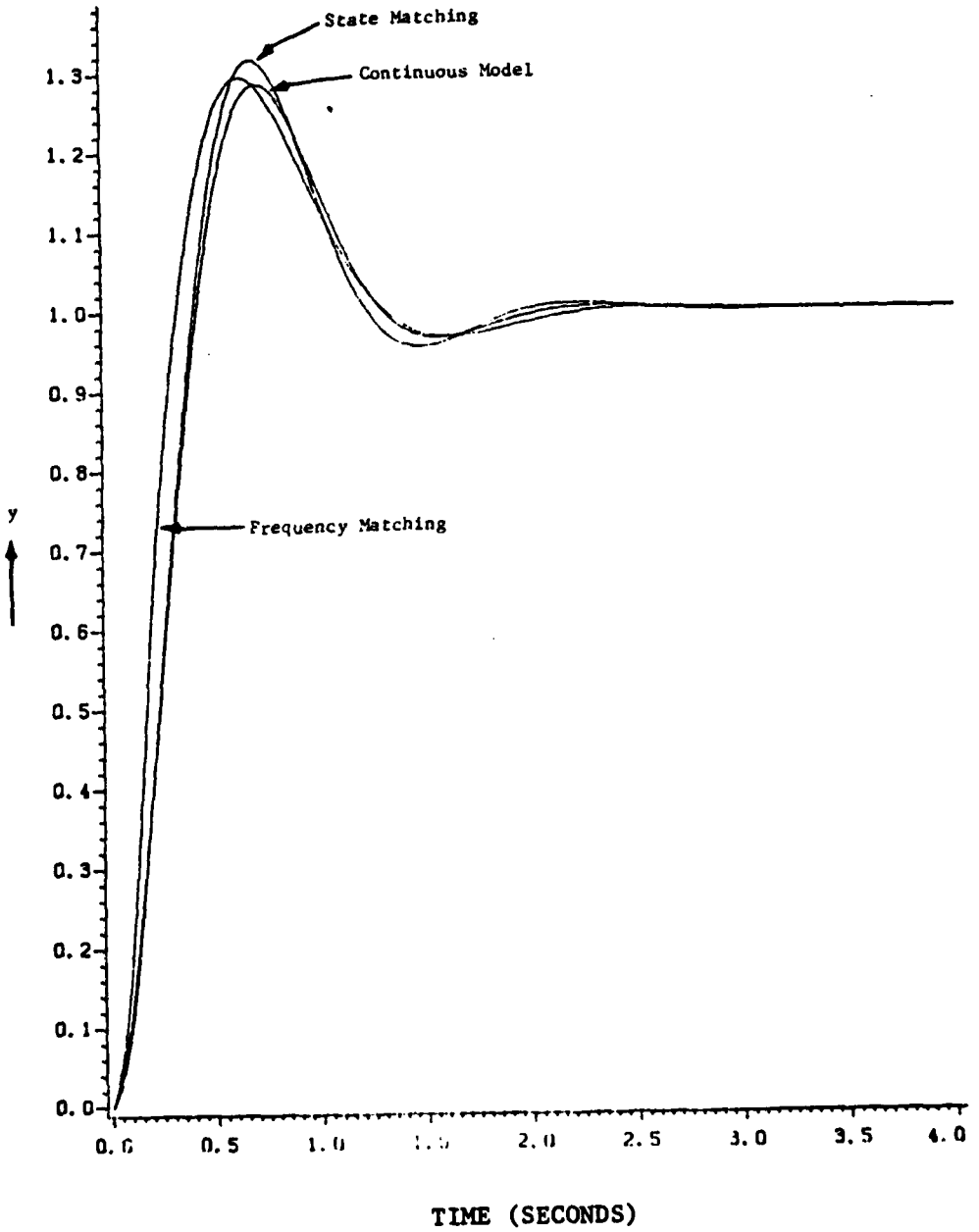

Figure 12. Comparison of Unit-Step Responses of Example 2 for T = 0.15

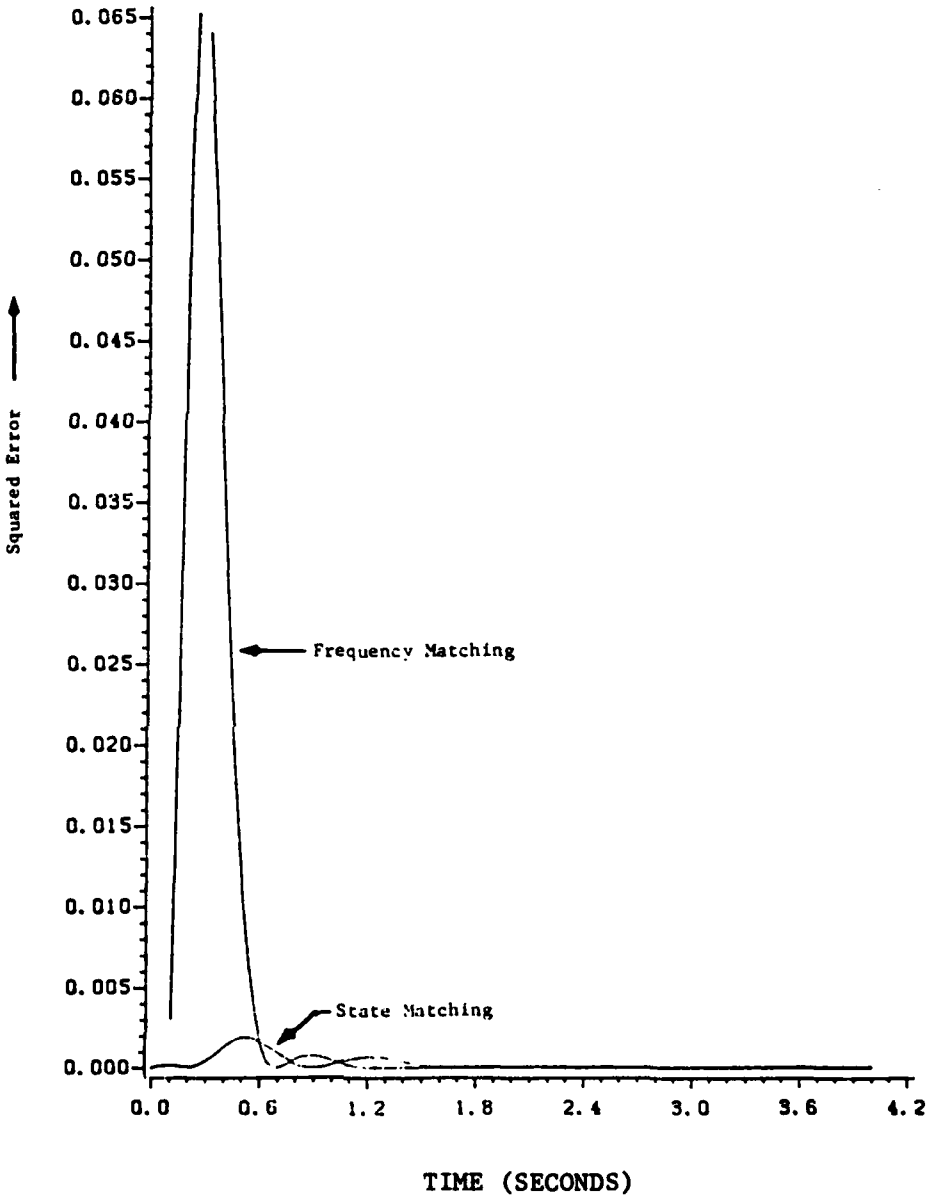

Figure 13. Squared Errors (Relative to the Continuous Model) of the Time Responses of Figure 12

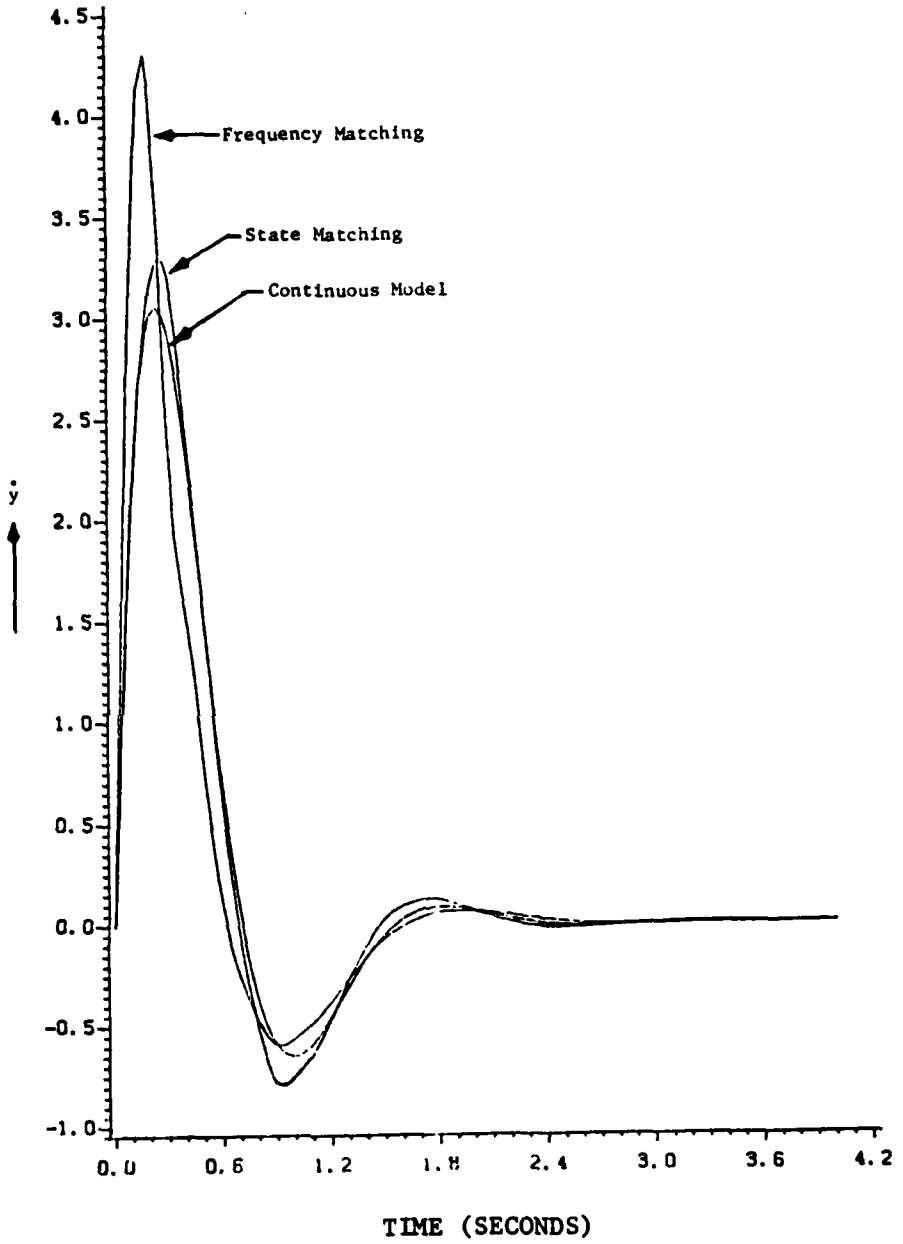

Figure 14. Unit-Step Responses of the Second State Variable of Example 2 at T = 0.15

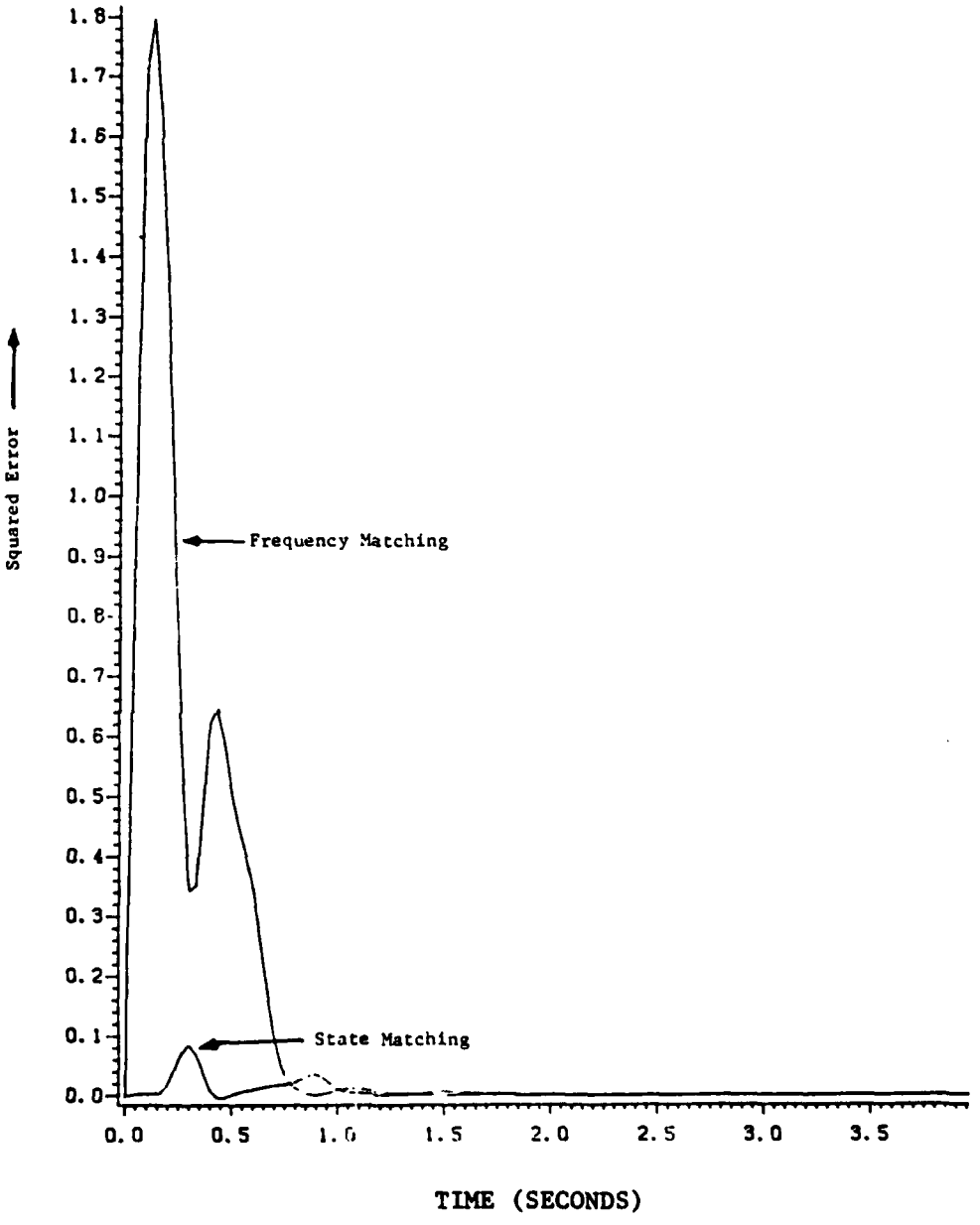

Figure 15. Squared Errors (Relative to the Continuous Model) of the Time Responses of Figure 14

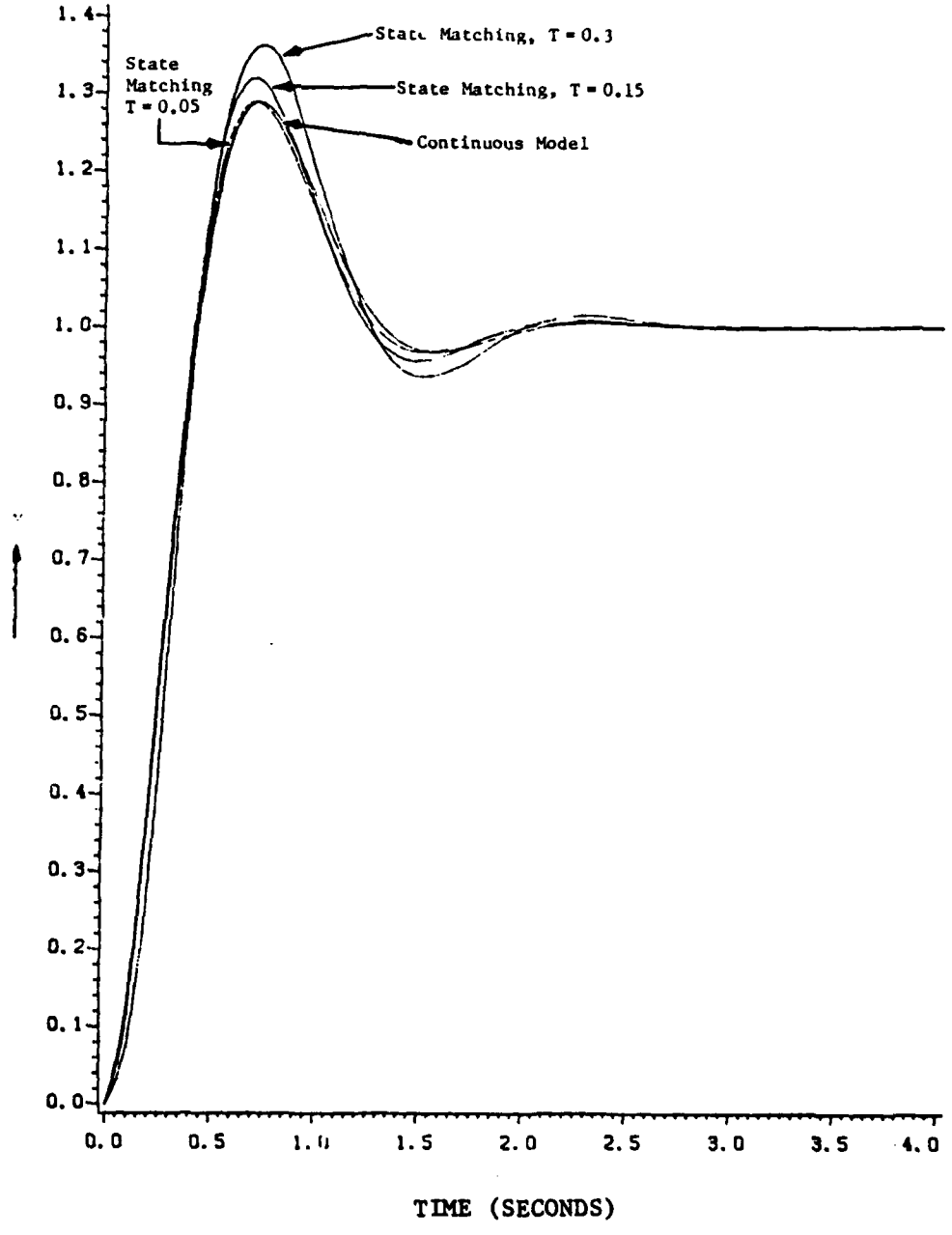

Figure 16. Unit-Step Responses of the State-Trajectory-Matching Design of Example 2 for Different Sampling Frequencies

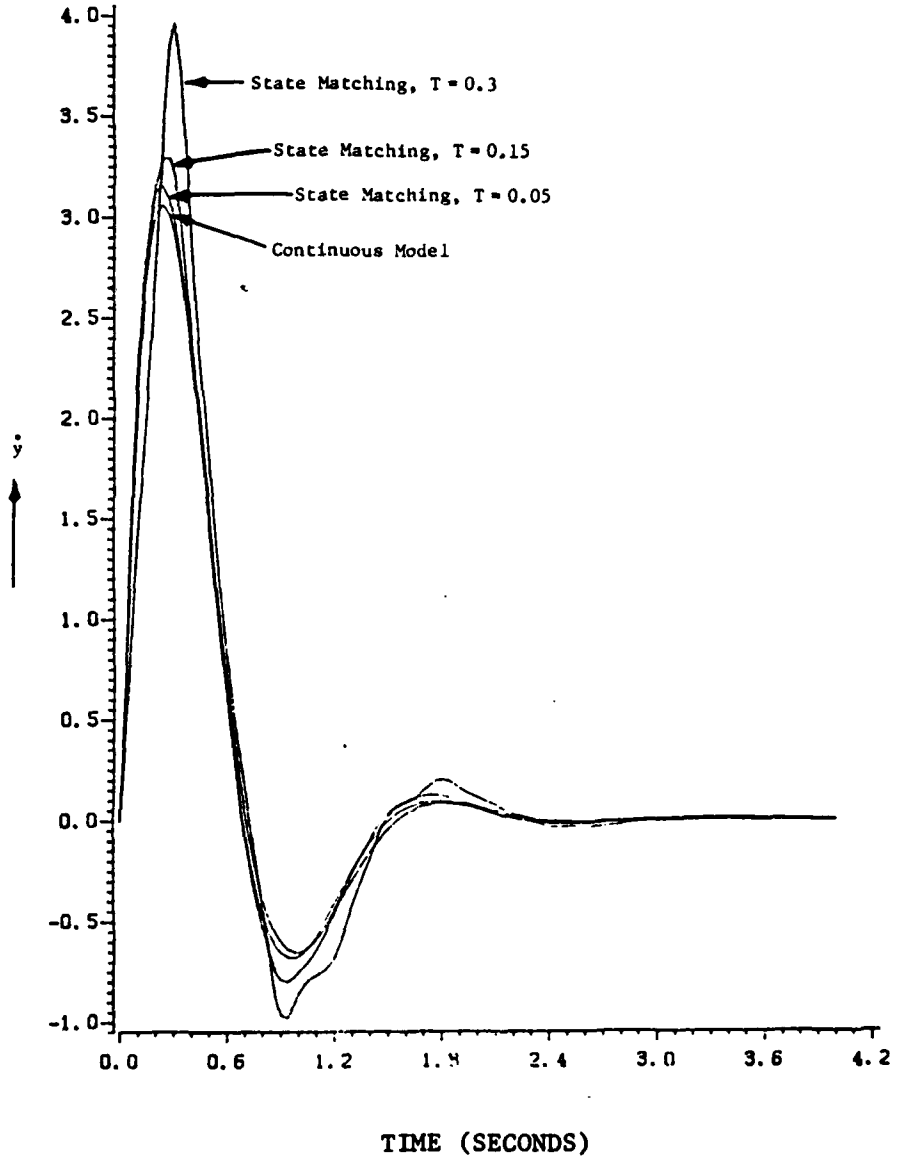

Figure 17. Unit-Step Responses of the Second State Variable $\dot{y}$ of the State-Trajectory-Matching Design of Example 2 for Different Sampling Frequencies

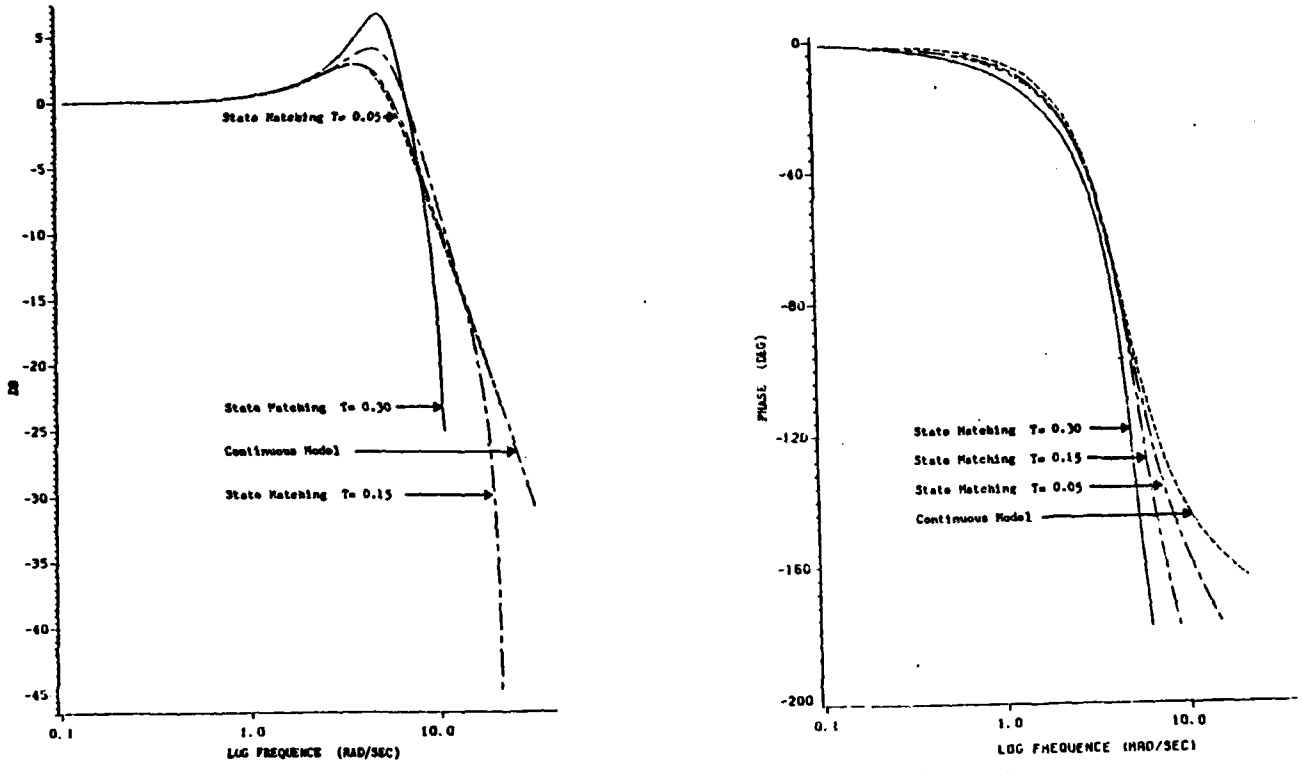

(a) DB vs omega

(b) phase vs omega

Figure 18. Frequency Response Comparison for the Frequency Matching Design of Example 2 at Different Sampling Frequencies

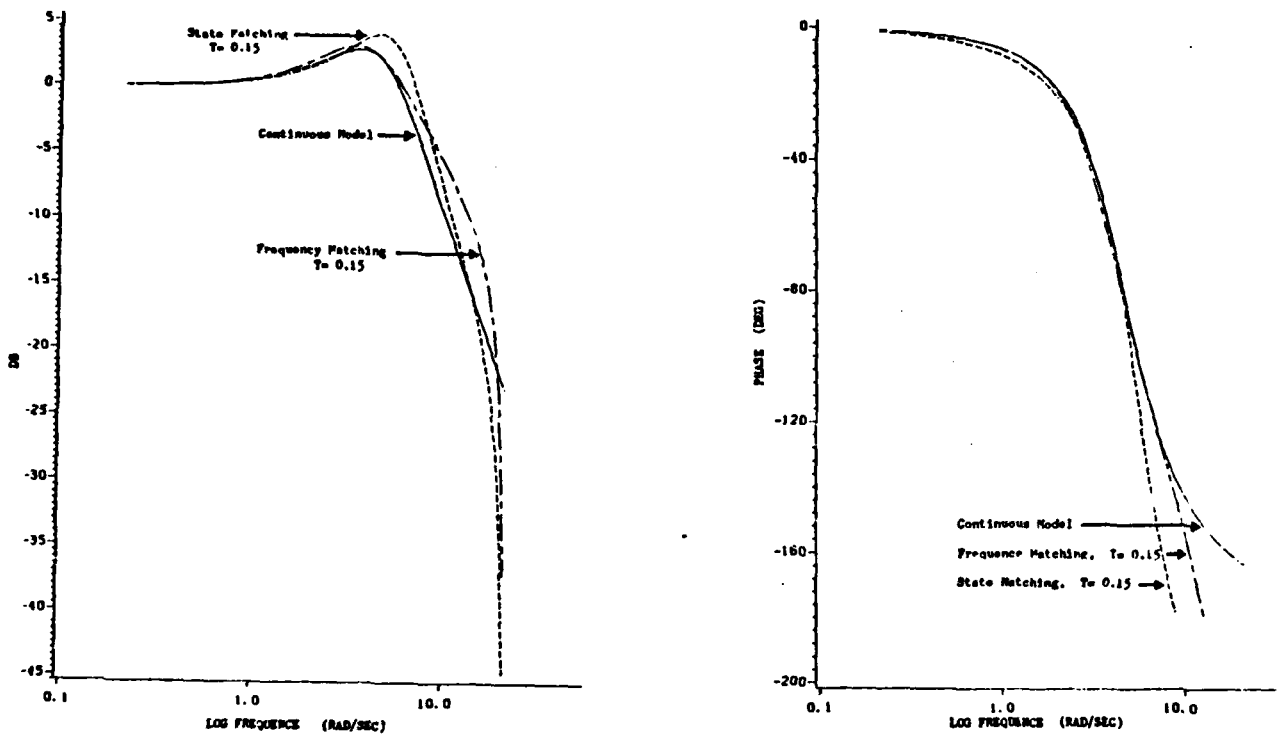

(a) DB vs omega

(b) phase vs omega

Figure 19. Frequency Response Comparison for Two Different Designs of Example 2 for Sampling Period T = 0.15 sec.

SECTION VI

VERIFICATION OF THE OPTIMAL CONTROL SEQUENCE VIA THE DISCRETE MAXIMUM PRINCIPLE

It has been shown in Section III that the extended maximum principle offers an efficient way to derive the optimal control sequence for a sampled-data system. The extended maximum principle, though powerful in this and many other applications [5-9] has not been widely used in the technical community. In many cases where the extended maximum principle may be used, an equivalent discrete performance index is derived and the discrete maximum principle is used instead [12-14].

It will be shown in this Section that the optimal control sequence of Eq. (42) may be derived by using the discrete maximum principle but a more cumbersome procedure is involved.

The performance index (5) may be written as

$$J = \lim_{N\to\infty} \frac{1}{2} \sum_{k=0}^{N-1} \int_{kT}^{(k+1)T} [\underline{x}'(t)Q\underline{x}(t) - 2\underline{x}'(t)Q\underline{x}_a(t) + \underline{x}_a'(t)Q\underline{x}_a(t)$$

$$+ \beta u^2(t) - 2\beta u(t)u_m(t) + \beta u_m^2(t)]dt \tag{129}$$

Since u(t) is the output of a zero-order-hold, substituting (10), (28), (30) into (129) (except for the term $\underline{x}_a'(t)Q\underline{x}_a(t)$) gives:

$$J = \lim_{N\to\infty} \frac{1}{2} \sum_{k=0}^{N-1} \{\underline{x}'(kT)[\hat{Q}(T)\underline{x}(kT) + 2M(T)\underline{b}u(kT)$$

$$- 2\hat{Q}_m(T)x_m(kT) - 2M_m(T)\underline{b}_m\alpha] + \hat{\beta}(T)u^2(kT)$$

$$- 2u(kT)[\underline{b}'\tilde{M}_m(T)\underline{x}_m(kT) + \beta_m(T)\alpha + \beta \int_{kT}^{(k+1)T} u_m(t)dt]$$

$$+ \int_{kT}^{(k+1)T} \underline{x}_a(t)Q\underline{x}_a(t) + \beta \int_{kT}^{(k+1)T} u_m^2(t)dt\} \tag{130}$$

where

$$\hat{Q}(T) = \int_0^T \Phi'(t)Q\Phi(t)dt \tag{131}$$

$$M(T) = \int_0^T \Phi'(t)Q\Phi^S(t)dt \tag{132}$$

$$\hat{\beta}(T) = \beta T + \underline{b}' \int_0^T \Phi^{S'}(t)Q\Phi^S(t)dt \tag{133}$$

$$\hat{Q}_m(T) = \int_0^T \Phi'(t)Q_m\Phi_m(t)dt \tag{134}$$

$$M_m(T) = \int_0^T \Phi'(t)Q_m\Phi_m^S(t)dt \tag{135}$$

$$\tilde{M}_m(T) = \int_0^T \Phi^{S'}(t)Q_m\Phi_m(t)dt \tag{136}$$

$$\beta_m(T) = \underline{b}' \int_0^T \Phi^{S'}(t)Q_m\Phi_m^S(t)dt\underline{b}_m \tag{137}$$

The discrete time system to be optimized is described by (47), which is repeated here for convenience:

$$x[(k+1)T] = \Phi(T)\underline{x}(kT) + \Phi^S(T)\underline{b}u(kT) \tag{138}$$

In the formulation of discrete maximum principle, the Hamiltonian is given by [12] (for the sake of notational brevity, the sampling period T is dropped in the argument of the discrete-time functions):

$$\begin{aligned} H(k) &= H(\underline{x}(k), \underline{p}(k+1), u(k)) \\ &= \underline{p}'(k+1)[\Phi(T)\underline{x}(k) + \Phi^S(T)\underline{b}u(k)] \\ &+ \frac{1}{2}x'(k)[\hat{Q}(T)\underline{x}(k) + 2M(T)\underline{b}u(k) - 2\hat{Q}_m(T)x_m(k) \\ &- 2M_m(T)\underline{b}_m\alpha] + \frac{1}{2}\hat{\beta}(T)u^2(k) - u(k)[\underline{b}'\tilde{M}_m(T)x_m(k) \end{aligned}$$

$$+ \beta_m(T)\alpha + \beta \int_{kT}^{(k+1)T} u_m(t)dt] + \frac{1}{2} \int_{kT}^{(k+1)T} x_a(t)Qx_a(t)dt$$

$$+ \frac{1}{2} \beta \int_{kT}^{(k+1)T} u_m^2(t)dt \tag{139}$$

The difference equation for the adjoint vector is

$$\underline{p}(k) = \frac{\partial H(k)}{\partial \underline{x}(k)}$$

$$= \hat{Q}(T)\underline{x}(k) + M(T)\underline{b}u(k) - \hat{Q}_m x_m(k)$$

$$- M_m(T)\underline{b}_m\alpha + \Phi'(T)\underline{p}(k+1) \tag{140}$$

The coupling equation, or the condition of optimality is given by

$$\frac{\partial H(k)}{\partial u(k)} = 0 \tag{141}$$

Substituting (139) into (141) gives

$$\underline{p}'(k+1)\Phi^s(T)\underline{b} + \underline{x}'(k)M(T)\underline{b} + \hat{\beta}(T)u(k)$$

$$- \underline{b}'\tilde{M}_m(T)\underline{x}_m(T) - \beta_m(T)\alpha - \beta \int_{kT}^{(k+1)T} u_m(t)dt = 0 \tag{142}$$

Solving the above equation for u(k) yields the optimal control sequence:

$$u(k) = \frac{1}{\hat{\beta}(T)} [\underline{b}'\tilde{M}_m(T)\underline{x}_m(k) - \underline{b}'M'(T)\underline{x}(k) + \beta_m(T)\alpha$$

$$- \underline{b}'\Phi^{s'}(T)\underline{p}(k+1) + \beta \int_{kT}^{(k+1)T} u_m(t)dt] \tag{143}$$

If it is recognized that

$$\Phi'(t) = \epsilon^{A'T} = \psi(-T) = [\psi(T)]^{-1} \tag{144}$$

then $p(k+1)$ may be obtained from (140) as

$$p(k+1) = \psi(T)[p(k) - \hat{Q}(T)\underline{x}(k) - M(T)\underline{b}u(k) + \hat{Q}_m(T)\underline{x}_m(k) + M_m(T)\underline{b}_m\alpha] \tag{145}$$

Also, in view of Eqs. (22), (29) and (31),

$$\int_{kT}^{(k+1)T} u_m(t)dt = \bar{c}_m\phi_m^s(T)\underline{x}_m(k) + \bar{c}_m\phi_m^{ss}(T)\underline{b}_m\alpha + d_m\alpha T \tag{146}$$

Substituting (145) and (146) into (143) and solving for $u(k)$ give the explicit expression of the optimal control sequence $u(k)$ as

$$\begin{aligned} u(k) = \frac{1}{\hat{\beta}(T) - \underline{b}'\phi^{s'}(T)\psi(T)M(T)\underline{b}} \{ & -\underline{b}'\phi^{s'}(T)\psi(T)p(k) \\ & + [-\underline{b}'M'(T) + \underline{b}'\phi^{s'}(T)\psi(T)\hat{Q}(T)]\underline{x}(k) \\ & + [\underline{b}'\tilde{M}_m(T) + \beta\bar{c}_m\phi_m^s(T) - \underline{b}'\phi^{s'}(T)\psi(T)\hat{Q}_m(T)]\underline{x}_m(k) \\ & + [\beta_m(T) + \beta\bar{c}_m\phi_m^{ss}(T)\underline{b}_m + \beta d_m T - \underline{b}'\phi^{s'}(T)\psi(T)M_m(T)\underline{b}_m]\alpha\} \end{aligned} \tag{147}$$

It remains to be shown that the right-hand side of (147) is equal to the right-hand side of (42). First, some preparation is in order. It is seen that, in view of (132) and (144)

$$\begin{aligned} M'(T) &= \int_0^T \int_0^\tau \psi(-\lambda)d\lambda Q\Phi(\tau)d\tau \\ &= \int_0^T \int_0^\tau \psi(x-\tau)dx Q\Phi(\tau)d\tau \\ &= \int_0^T \int_x^T \psi(x-\tau)Q\Phi(\tau)d\tau dx \end{aligned} \tag{148}$$

Note that a change of variables and a change of order of integrations are involved in obtaining the last expression in (148). Furthermore, it is seen from (38) and (39) that

$$F^{s}(T) = \int_0^T \int_0^x \psi(x - \tau) Q\Phi(\tau) d\tau dx \tag{149}$$

Thus

$$\begin{aligned} F^{s}(T) + M'(T) &= \int_0^T \int_0^T \psi(x - \tau) Q\Phi(\tau) d\tau dx \\ &= \int_0^T \psi(x - T) \int_0^T \psi(T - \tau) Q\Phi(\tau) d\tau dx \\ &= \int_0^T \psi(-\lambda) F(T) d\lambda \\ &= \Phi^{s'}(T) F(T) \end{aligned} \tag{150}$$

Therefore

$$F^{s}(T) = -M'(T) + \Phi^{s'}(T) F(T) \tag{151}$$

Now changing the order of integration in the first expression of $M'(T)$ in (148), with the aid of (144) and (132), gives

$$\begin{aligned} M'(T) &= \int_0^T \int_0^\tau \psi(-\lambda) d\lambda Q\Phi(\tau) d\tau \\ &= \int_0^T \int_\lambda^T \psi(-\lambda) Q\Phi(\tau) d\tau d\lambda \\ &= \int_0^T \psi(-\lambda) Q \int_\lambda^T \Phi(\tau) d\tau d\lambda \\ &= \int_0^T \psi(-\lambda) Q \int_0^T \Phi(\tau) d\tau d\lambda - \int_0^T \psi(-\lambda) Q \int_0^\lambda \Phi(\tau) d\tau d\lambda \end{aligned}$$

$$= \phi^{s'}(T)Q\phi^{s}(T) - \int_0^T \psi(-\lambda)Q\phi^{s}(\lambda)d\lambda$$

$$= \phi^{s'}(T)Q\phi^{s}(T) - M(T) \tag{152}$$

Substituting (152) into (151) gives

$$F^{s}(T) = -\phi^{s'}(T)Q\phi^{s}(T) + \phi^{s'}(T)F(T) + M(T) \tag{153}$$

But since $\psi(T)$ is a matrix exponential, M(T) may be expressed in the following form, with the aid of the theorem given in Appendix C:

$$M(T) = \int_0^T \phi'(t)Q\phi^{s}(t)dt$$

$$= \psi(-T) \int_0^T \psi(T - t)Q \int_0^t \phi(\lambda)d\lambda dt$$

$$= \psi(-T) \int_0^T \int_0^t \psi(t - \tau)Q\phi(\tau)d\tau dt$$

$$= \psi(-T) \int_0^T F(t)dt = \psi(-T)F^{s}(T) \tag{154}$$

Hence, in view of (144) and (154), $F^{s}(T)$ of (153) may be written as:

$$F^{s}(T) = -\phi^{s'}(T)Q\phi^{s}(T) + \phi^{s'}(T)F(T) + \phi'(T)F^{s}(T) \tag{155}$$

Integrating both sides of (155) from 0 to T gives

$$F^{ss}(T) = -\int_0^T \phi^{s'}(t)Q\phi^{s}(t)dt + \phi^{s'}(T)F^{s}(T) \tag{156}$$

Now it can be shown that the control sequence given in (147) is identical to that given in (42). With the aid of (133), (154) and (156) the

denominator in the right-hand side of (147) may be reduced as follows:

$$\hat{\beta}(T) - \underline{b}'\Phi^{s'}(T)\psi(T)M(T)\underline{b}$$

$$= \beta T + \underline{b}'[\int_0^T \Phi^{s'}(t)Q\Phi^{s}(t)dt - \Phi^{s'}(T)\psi(T)M(T)]\underline{b}$$

$$= \beta T + \underline{b}'[\int_0^T \Phi^{s'}(t)Q\Phi^{s}(t)dt - \Phi^{s'}(T)F^{s}(T)]\underline{b}$$

$$= \beta T - \underline{b}'F^{ss}(T)\underline{b} \tag{157}$$

Because $\psi(T)$ is a matrix exponential, the coefficient of $\underline{p}(kT)$ in (147) may be reduced as follows:

$$\Phi^{s'}(T)\psi(T) = \int_0^T \psi(-t)dt\psi(T) = \int_0^T \psi(T - t)dt$$

$$= \int_0^T \psi(\lambda)d\lambda = \psi^{s}(T) \tag{158}$$

The coefficient of $\underline{x}(k)$ may be reduced as follows:

$$-M'(T) + \Phi^{s'}(T)\psi(T)\hat{Q}(T)$$

$$= -M'(T) + \Phi^{s'}(T)\psi(T)\int_0^T \psi(-t)Q\Phi(t)dt$$

$$= -M'(T) + \Phi^{s'}(T)F(T) = F^{s}(T) \tag{159}$$

where (131), (38) and (151) have been used. Similarly the coefficient of $\underline{x}_m(k)$ in (147) is shown to be

$$\underline{b}'\tilde{M}_m(T) + \beta\bar{c}_m\Phi_m^{s}(T) - \underline{b}'\Phi^{s'}(T)\psi(T)\tilde{Q}_m(T)$$

$$= \beta\bar{c}_m\Phi_m^{s}(T) - \underline{b}'F_m^{s}(T) \tag{160}$$

For the coefficient of α in (147), it is seen that

$$\beta_m(T) - \underline{b}'\Phi^{s'}(T)\psi(T)M_m(T)\underline{b}_m$$

$$= \underline{b}'\left[\int_0^T \Phi^{s'}(t)Q_m\Phi_m^s(t)dt - \Phi^{s'}(T)F_m^s(T)\right]\underline{b}_m$$

$$= -\underline{b}'F_m^{ss}(T)\underline{b}_m \tag{161}$$

Where formulas (135), (40), (137) and an equivalent of (156) for $F_m^{ss}(T)$ have been used.

Finally, the following relations (which have been found in the derivations of (154) - (161))

$$\psi(T)\hat{Q}(T) = F(T) \tag{162}$$

$$\psi(T)M(T) = F^s(T) \tag{163}$$

$$\psi(T)\hat{Q}_m(T) = F_m(T) \tag{164}$$

$$\psi(T)M_m(T) = F_m^s(T) \tag{165}$$

lead to the fact that the solution $\underline{p}(k)$ of (145) is the negative of the solution of the difference equation given by (49). This fact and Eqs. (157) - (161) imply that the optimal control sequence given in (147) by the discrete maximum principle is identical to the optimal control sequence given in (42) by the extended maximum principle. It is also clear that the derivation of (42) is much simpler than the derivation of (147). The extended maximum principle even yields more concise expressions.

SECTION VII

CONCLUSIONS AND RECOMMENDATIONS

The extended maximum principle has been applied to the problem of designing a digital controller that drives the state trajectory of a continuous plant in an output feedback system to follow its continuous model as closely as possible. Closed form expressions of the optimal digital controller have been obtained, as given by Equations (74), (76), (90) and (95). The result has been verified by a derivation via the widely used discrete maximum principle, which would entail a far more cumbersome procedure to obtain the same result.

The optimal digital controller gives rise to a closed-loop system (Fig. 2 or Fig. 4) that has a discrete transfer function equal to (Eq. (82) repeated here):

$$\frac{Y(z)}{R(z)} = \frac{\underline{b}'H_m(z)\underline{b}_m}{\underline{b}'H(z)\underline{b}} \overline{G_h G}(z) \tag{166}$$

if $\beta = 0$ (integral squared error of the control signal is not weighted in the performance index). A similar expression may be derived for $\beta \neq 0$. The formulas for the digital controller, given by (74), (76), (90) and (95), are rather difficult to compute. Numerical computations of these equations always result in poles and zeros in the unstable region that should not be implemented. Owing to the amount of computations involved, it is not clear whether the unstable poles and zeros in the digital controller should be identical to one another and thus be cancelled, or are introduced by z-transforming the control and error sequences. More study is needed in this direction.

For the lower order systems (second and third order systems), this method of digital controller design yields excellent results, even though the sampling frequencies are relatively low. The digital controllers designed by the present method compares favorably with those designed by the frequency matching method, and are far superior to those obtained by the conventional Tustin or impulse invariant transformations.

Attempts have also been made to compute the digital controller of Eq. (95) for a sixth order model of the inner loop of the longitudinal control of YF-16 fighter aircraft at 30,000 ft altitude and Mach 0.6. It is found that (95) is not well conditioned for numerical computation for higher order systems in the sense that it involves ratios of differences between polynomials which are approximately equal to one another. This and the fact that a large amount of multiplication and integration are required in computing $H(z)$ and $H_m(z)$ make it impossible to obtain a valid expression of the digital controller by way of the computer programs available to or developed in this project. Another difficulty involved in computing (95) is the high order in the resulting transfer function. The ill-conditionedness of the digital controller formulas may perhaps be circumvented by transforming the z-plane formulas into the w'-plane, i.e.,

$$z = \frac{1 + w' \frac{T}{2}}{1 - w' \frac{T}{2}} \tag{167}$$

The w'-plane concept was initiated by Whitbeck [16]. W'-transformation has the advantage over the w transformation in that when $T \to 0$, $w' \to s$. It may also be easier to find reduced-order models of the digital controller in the w'-plane in order for this method to apply to practical higher order systems.

Equation (166) represent the ideal closed-loop transfer function when the optimal digital controller is employed. It represents the best closed-loop digital control system that can be achieved if the digital system is required to model after the continuous system.

The numerical computation of the optimal digital controller transfer function of Eqs. (74), (76), (90) and (95) involves integrations and double integrations of matrix exponentials and of convolutions of matrix exponentials. We used Romberg's algorithm [17] on an IBM 370 computer with extended precision. For a sixth order system, the CPU time required to compute a set of coefficients for (76) is 0.25646 hours for $T = 0.04$, and 0.74129 hours for $T = 0.1$. Therefore, a more efficient computer program

such as one that performs analytic integration by giving $\frac{1}{a} \epsilon^{at}$ as the integration of ϵ^{at} for matrix functions needs to be developed. The analytic integration program would not only cut down the CPU time, but also improves precision since numerical values are substituted at the last stage. It is useful not only for computing the formulas of the digital controller developed in this project, but also in discretizing a continuous control system or in applying the discrete maximum principle to sampled-data systems.

REFERENCES

1. K. S. Rattan and H. H. Yeh, "Discretizing Continuous Data Control Systems," Computer Aided Design, Vol. 10, No. 5, September 1978, pp. 299-306.

2. K. S. Rattan, "Digitalization of Existing Continuous Data Control Systems," AFWAL-TM-80-105-FIGC, September 1980 (Technical Memorandum), Flight Dynamics Laboratory, Wright-Patterson Air Force Base, Ohio 45433.

3. H. H. Yeh and C. S. Yeh, "On the Digital Controller Design for Point-by-point Output Matching," 10th Annual Southeastern Symposium on System Theory, Mississippi State University, March 1978.

4. S. S. L. Chang, "A General Theory of Optimal Processes," SIAM Journal of Control, Series A, Vol. 4, 1966, pp. 46-55.

5. H. H. Yeh, "An Extension of Pontryagin's Maximum Principle," Ph.D. Dissertation, Department of Electrical Engineering, Ohio State University, 1967.

6. H. H. Yeh and J. T. Tou, "On the General Theory of Optimal Processes," International Journal of Control, Vol. 9, No. 4, April 1969, pp. 433-451.

7. H. H. Yeh and Wyle Y. W. Tsan, "Optimal Synthesis of Saturating Sampled-data Systems Using Integral Performance Index," International Journal of Control, Vol. 14, No. 1, July 1971, pp. 33-42.

8. H. H. Yeh, "Optimal Control with Partially Specified Input Functions," International Journal of Control, Vol. 16, No. 1, 1972, pp. 71-80.

9. H. H. Yeh and R. J. Kuhler, "Additional Properties of an Extended Maximum Principle," International Journal of Control, Vol. 17, No. 6, 1973, pp. 1281-1286.

10. H. H. Yeh, "Optimal Design of Digital Flight Control Systems Following an Analog Model," 1981 USAF-SCEEE Summer Faculty Research Program, F49620-79-C-0038, Aug 14, 1981.

11. J. J. D'Azzo and C. H. Houpis, Linear Control System Analysis and Design, McGraw Hill, 1975, 1981.

12. B. C. Kuo, Digital Control Systems, Holt, Rinehart and Winston, 1980, Chapter 12, p. 609.

13. Gran, R., Berman, H., and Rossi, M., "Optimal Digital Flight Control for Advanced Fighter Aircraft," Journal of Aircraft, Vol. 14, No. 1, January 1977, pp. 32-37.

14. Glasson, D. P., "Research in Multirate Estimation and Control," TR-1356-1, The Analytic Sciences Corporation, Dec. 20, 1980 (Prepared for the Office of Naval Research N00014-79-C-0431).

15. Rattan, K. S., "Computer-Aided Design of Sampled-Data Control Systems via Complex Curve Fitting," Ph.D. Dissertation, University of Kentucky, Lexington, Kentucky, 1975.

16. R. F. Whitbeck and L. G. Hoffman, "Analysis of Digital Flight Control Systems with Flying Quality Applications," Vol. II, Technical Report AFFDL-TR-78-115, 1978.

17. Brice Carnhan, H. A. Luther and James O. Wilkes, Applied Numerical Methods," John Wiley & Sons, Inc., 1969, p. 91-94.

APPENDIX A

THE OVERALL STATE EQUATIONS OF THE CONTINUOUS MODEL

The feedback structure in Fig. 1 gives

$$e_m(t) = r(t) - y_m(t) \tag{A-1}$$

Eliminating $e_m(t)$ and $y_m(t)$ among Eqs. (A-1), (2) and (4) and solving for $u_m(t)$ gives

$$u_m(t) = \frac{-d_c\bar{c}}{1+dd_c}\underline{x}_a(t) + \frac{\bar{c}_c}{1+dd_c}\underline{x}_c(t) + \frac{d_c}{1+dd_c}r(t) \tag{A-2}$$

Eliminating $u_m(t)$ and $y_m(t)$ among Eqs. (A-1), (2) and (4) and solving for $e_m(t)$ gives

$$e_m(t) = \frac{-\bar{c}}{1+dd_c}\underline{x}_a(t) + \frac{-d\bar{c}_c}{1+dd_c}\underline{x}_c(t) + \frac{1}{1+dd_c}r(t) \tag{A-3}$$

Substituting (A-2) into (1) and (A-3) into (3) yields, respectively,

$$\dot{\underline{x}}_a(t) = \left(A - \frac{\underline{b}d_c\bar{c}}{1+dd_c}\right)\underline{x}_a(t) + \frac{\underline{b}\bar{c}_c}{1+dd_c}\underline{x}_c(t) + \frac{\underline{b}d_c}{1+dd_c}r(t) \tag{A-4}$$

$$\dot{\underline{x}}_c(t) = \frac{-b_c\bar{c}}{1+dd_c}\underline{x}_a(t) + \left(A_c - \frac{b_c d\bar{c}_c}{1+dd_c}\right)\underline{x}_c(t) + \frac{b_c}{1+dd_c}r(t) \tag{A-5}$$

APPENDIX B

SOLUTIONS OF THE STATE AND ADJOINT EQUATIONS

The solution $\underline{p}(t)$ of Eq. (14), in terms of $\underline{x}(t)$ and $\underline{x}_a(t)$, is given by

$$\underline{p}(t) = \psi(t-kT)\underline{p}(kT) + \int_{kT}^{t} \psi(t-\tau)Q[\underline{x}(\tau) - \underline{x}_a(\tau)]d\tau \tag{B-1}$$

for $kT < t \leq kT$, where

$$\psi(t-kT) = \epsilon^{-A'(t-kT)} \tag{B-2}$$

With the aid of Eq. (28), Eq. (B-1) can be written as

$$\underline{p}(t) = \psi(t-kT)\underline{p}(kT) + \int_{kT}^{t} \psi(t-\tau)Q\underline{x}(\tau)d\tau$$

$$- \int_{kT}^{t} \psi(t-\tau)Q\underline{x}_m(\tau)d\tau \tag{B-3}$$

The vectors $\underline{x}_m(t)$ and $\underline{x}(t)$ are solutions of Eq. (21) and Eq. (7), respectively. They are given by, for $kT < t \leq (k+1)T$,

$$\underline{x}_m(t) = \Phi_m(t-kT)\underline{x}_m(kT) + \Phi_m^s(t-kT)\underline{b}_m\alpha \tag{B-4}$$

$$\underline{x}(t) = \Phi(t-kT)\underline{x}(kT) + \Phi^s(t-kT)\underline{b}u(kT) \tag{B-5}$$

where

$$\Phi_m(t-kT) = \epsilon^{A_m(t-kT)} \tag{B-6}$$

$$\Phi_m^s(t-kT) = \int_{kT}^{t} \Phi_m(t-\tau)d\tau = \int_{0}^{t-kT} \Phi_m(\tau)d\tau \tag{B-7}$$

$$\Phi(t-kT) = \epsilon^{A(t-kT)} \tag{B-8}$$

$$\Phi^s(t-kT) = \int_{kT}^{t} \Phi(t-\tau)d\tau = \int_{0}^{t-kT} \Phi(\tau)d\tau \qquad \text{(B-9)}$$

Now substituting (B-4) and (B-5) into (B-3) and invoking (B-7) and (B-9) gives, for $kT < t \leq (k+1)T$,

$$\begin{aligned} \underline{p}(t) = \psi(t-kT)\underline{p}(kT) &+ \int_{kT}^{t} \psi(t-\tau)Q\Phi(\tau-kT)d\tau\underline{x}(kT) \\ &+ \int_{kT}^{t} \psi(t-\tau)Q \int_{kT}^{\tau} \Phi(\tau-\lambda)d\lambda d\tau \underline{b}u(kT) \\ &- \int_{kT}^{t} \psi(t-\tau)Q_m\Phi_m(\tau-kT)d\tau\underline{x}_m(kT) \\ &- \int_{kT}^{t} \psi(t-\tau)Q_m \int_{kT}^{\tau} \Phi_m(\tau-\lambda)d\lambda d\tau \underline{b}_m\alpha \end{aligned} \qquad \text{(B-10)}$$

In view of the identities derived in Appendix C, a new set of notations may be used for the integrals which appear in the above equation, for the sake of clarity:

$$\begin{aligned} \underline{p}(t) = \psi(t-kT)\underline{p}(kT) &+ F(t-kT)\underline{x}(kT) + F^s(t-kT)\underline{b}u(kT) \\ &- F_m(t-kT)\underline{x}_m(kT) - F_m^s(t-kT)\underline{b}_m\alpha \end{aligned} \qquad \text{(B-11)}$$

where

$$\begin{aligned} F(t-kT) &= \int_{kT}^{t} \psi(t-\tau)Q\Phi(\tau-kT)d\tau \\ &= \int_{0}^{t-kT} \psi(t-kT-\tau)Q\Phi(\tau)d\tau \end{aligned} \qquad \text{(B-12)}$$

$$F^S(t-kT) = \int_{kT}^{t} \psi(t-\tau) Q \int_{kT}^{\tau} \phi(\tau-\lambda) d\lambda d\tau$$

$$= \int_{0}^{t-kT} \int_{0}^{\tau} \psi(\tau-\lambda) Q \phi(\lambda) d\lambda d\tau$$

$$= \int_{0}^{t-kT} F(\tau) d\tau \qquad \text{(B-13)}$$

$$F_m(t-kT) = \int_{kT}^{t} \psi(t-\tau) Q_m \phi_m(\tau-kT) d\tau$$

$$= \int_{0}^{t-kT} \psi(t-kT-\tau) Q_m \phi_m(\tau) d\tau \qquad \text{(B-14)}$$

$$F_m^S(t-kT) = \int_{kT}^{t} \psi(t-\tau) Q_m \int_{kT}^{\tau} \phi_m(\tau-\lambda) d\lambda d\tau$$

$$= \int_{0}^{t-kT} \int_{0}^{\tau} \psi(\tau-\lambda) Q_m \phi_m(\lambda) d\lambda d\tau$$

$$= \int_{0}^{t-kT} F_m(\tau) d\tau \qquad \text{(B-15)}$$

APPENDIX C

FORMULAS OF FINITE MULTIPLE INTEGRALS

THEOREM: The convolution between $f(t)$ and the area under $g(t)$, if it exists, is equal to the area under the convolution between $f(t)$ and $g(t)$.

$$\int_0^T f(T-\tau) \int_0^\tau g(\lambda)d\lambda d\tau = \int_0^T \int_0^t f(t-\tau)g(\tau)d\tau dt \qquad \text{(C-1)}$$

Proof.

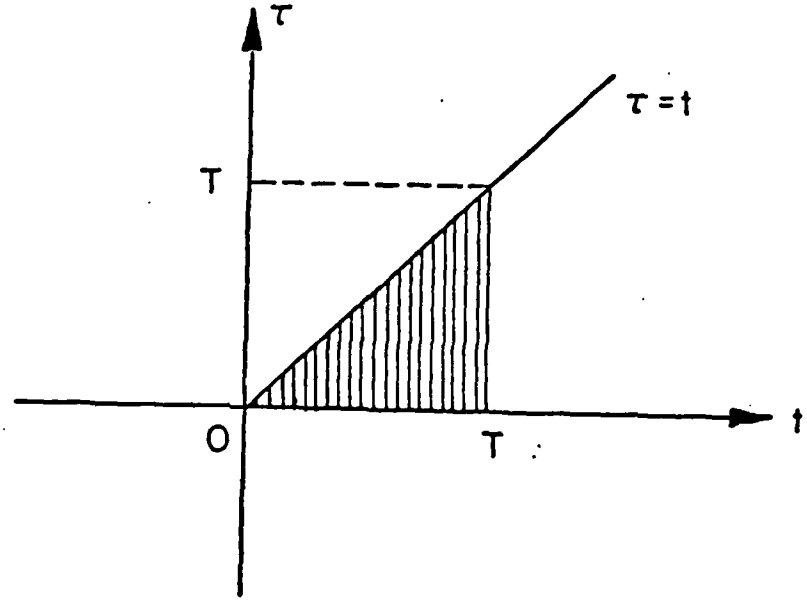

Fig. C-1. Area of integration in (t,τ) plane.

In view of Fig. C-1, interchanging the order of integration for the integral in the right-hand side of Eq. (C-1) gives

$$\int_0^T \int_0^t f(t-\tau)g(\tau)d\tau dt = \int_0^T \int_\tau^T f(t-\tau)g(\tau)dtd\tau \qquad \text{(C-2)}$$

Substituting t' for t-τ and dt' for dt (regarding τ as a constant in the partial integration with respect to t) in Eq. (C-2), we obtain, after changing the integration limits accordingly,

$$\int_0^T \int_\tau^T f(t-\tau)g(\tau)dtd\tau = \int_0^T \int_0^{T-\tau} f(t')dt'g(\tau)d\tau \qquad \text{(C-3)}$$

In a similar fashion, interchanging the order of integration in the left-hand side of Eq. (C-1) gives

$$\int_0^T f(T-\tau) \int_0^\tau g(\lambda)d\lambda d\tau = \int_0^T \int_\lambda^T f(T-\tau)g(\lambda)d\tau d\lambda \qquad \text{(C-4)}$$

Substituting t for T-τ and dt for -dτ and changing the integration limits accordingly in the right-hand side of Eq. (C-4) gives

$$\int_0^T \int_\lambda^T f(T-\tau)g(\lambda)d\tau d\lambda = \int_0^T \int_{T-\lambda}^0 (-1)f(t)dtg(\lambda)d\lambda \qquad \text{(C-5)}$$

Comparison of the Eq. (C-3) with Eq. (C-5) completes the proof.

The following is a list of formulas that are used in the derivations in Appendix B. The proof involves changes of variables or changes of order of integrations, and is hence omitted.

Formula 1. $$\int_{kT}^{t} f(t-\tau)d\tau = \int_0^{t-kT} f(\tau)d\tau$$

Formula 2. $$\int_{kT}^{t} f(t-\tau)g(\tau-kT)d\tau = \int_0^{t-kT} f(t-kT-\tau)g(\tau)d\tau$$

Formula 3. $$\int_{kT}^{t} f(t-\tau) \int_{kT}^{\tau} g(\tau-\lambda)d\lambda d\tau = \int_0^{t-kT} f(t-kT-\tau) \int_0^{\tau} g(\lambda)d\lambda d\tau$$

Formula 4. $$\int_{kT}^{t} f(t-\tau) \int_{kT}^{\tau} g(\tau-\lambda)d\lambda d\tau = \int_0^{t-kT} \int_0^{\tau} f(\tau-\lambda)g(\lambda)d\lambda d\tau$$

Formula 5. $$\int_{kT}^{(k+1)T} \int_{kT}^{t} f(t-\tau)g(\tau-kT)d\tau dt = \int_0^T \int_0^t f(t-\tau)g(\tau)d\tau dt$$

Formula 6. $$\int_0^t f(t-\tau)\int_0^\tau g(\tau-\lambda)\,d\lambda\,d\tau = \int_0^t f(t-\tau)\int_0^\tau g(\lambda)\,d\lambda\,d\tau$$

Formula 7. $$\int_0^t f(t-\tau)\int_0^\tau g(\lambda)\,d\lambda\,d\tau = \int_0^t \int_0^\tau f(\tau-\lambda)g(\lambda)\,d\lambda\,d\tau$$

Formula 8. $$\int_0^t f(t-\tau)\int_0^\tau g(\tau-\lambda)\,d\lambda\,d\tau = \int_0^t \int_0^\tau f(\tau-\lambda)g(\lambda)\,d\lambda\,d\tau$$

Formula 9. $$\int_{kT}^{(k+1)T} \int_{kT}^{t} f(t-\tau) \int_{kT}^{\tau} g(\tau-\lambda)\,d\lambda\,d\tau\,dt$$

$$= \int_0^T \int_0^t f(t-\tau)\int_0^\tau g(\lambda)\,d\lambda\,d\tau\,dt$$

Formula 10. $$\int_{kT}^{(k+1)T} \int_{kT}^{t} f(t-\tau) \int_{kT}^{\tau} g(\tau-\lambda)\,d\lambda\,d\tau\,dt$$

$$= \int_0^T \int_0^t \int_0^\tau f(\tau-\lambda)g(\lambda)\,d\lambda\,d\tau\,dt$$

APPENDIX D

SUBALIASES IN THE FREQUENCY RESPONSE OF DIGITALLY CONTROLLED SOURCES

SUBALIASES IN THE FREQUENCY RESPONSE OF DIGITALLY CONTROLLED SYSTEMS

Hsi-Han Yeh*
University of Kentucky, Lexington, Ky.
and
Richard F. Whitbeck**
Systems Technology, Inc., Hawthorne, Calif.

I. INTRODUCTION

In a recent paper, Whitbeck, Didaleusky and Hofmann [1] extended the concept of the tradiational "sampled spectrum" frequency response for discretely excited continuous systems. When a sinusoidal wave is input to a discretely excited continuous system, N sine waves at different alias frequencies are required to match the continuous steady-state time response at the sampling instants and at N-1 equally spaced intersample points. In the special case of N=1, this reduces to the traditional concept of the sampled-spectrum frequency response for sampled-data systems. Letting N approach infinity gives an infinite spectrum for the continuous steady-state response of a discretely excited continuous system. This theory enables one to write an exact expression of the time response sampled at any rate that is an integer multiple of the sampling rate of the system. The practical value of knowing such an expression of the output is evident.

---

*Associate Professor, Department of Electrical Engineering

**Principal Research Engineer

However, in the derivation of Whitbeck, Didaleusky and Hofmann [1], only positive aliases of the input frequency are included in the representation of the sampled continuous output. Whereas the result is correct for the case where N is finite, the limit case where N approaches infinity is in error and it contains only half of the spectral components necessary for an asymptotic representation of the continuous output. In this paper, a new derivation which includes subaliases in the spectral representation of the sampled output will be presented. It will be shown that, as the output sampling rate N approaches infinity, the infinite spectrum of the continuous output contains all aliases and subaliases of the input frequency. Also presented will be a direct derivation of the infinite spectrum of the continuous output, without invoking the expression of the sampled steady-state response. This confirms the correct representation of the continuous steady-state output of discretely excited continuous systems in response to a single sinusoidal input. This derivation brings forth a unified concept of frequency response which enables one to write the spectral representation of the output of a discretely excited continuous system on the basis of the frequency response of the continuous system.

II. FREQUENCY COMPONENTS IN THE SAMPLED OUTPUT

Consider the system of Fig. 1 where G(s) represents an arbitrary transfer function and M(s) represents an arbitrary data hold. Let the input be a unit amplitude exponential ε^{jbt} and the output be sampled with period T/N. Using multirate sampling results (See Appendix of [1]) yields

$$C^{T/N} = \left[GMR^T\right]^{T/N} = (GM)^{T/N} R^T$$

$$= (GM)^{T/N} \frac{z^N}{z^N - \epsilon^{jbT}} \qquad (z \triangleq \epsilon^{sT/N}) \tag{1}$$

where the notation follows Whitbeck, Didaleusky and Hofmann [1]. The superscript denotes the period of sampling operation. In the time domain, a sampled function $[r(t)]^T$ or r^T is defined by

$$[r(t)]^T \triangleq \sum_{n=-\infty}^{\infty} r(n)\delta(t-nT) = r(t) \sum_{n=-\infty}^{\infty} \delta(t-nT) \tag{2}$$

In the s-domain, a sampled function R^T is defined by

$$R^T(s) \triangleq \sum_{n=0}^{\infty} r(n)\epsilon^{-nsT} = \frac{1}{T} \sum_{n=-\infty}^{\infty} R(s + j\frac{2\pi n}{T}) \tag{3}$$

and in z-domain,

$$R^T(z) \triangleq R^T(s)\Big|_{\epsilon^{sT}\to z} \tag{4}$$

But in the presence of a higher rate sampler with period T/N, as in this paper, it is desirable to use $z=\epsilon^{sT/N}$ and

$$R^T(z^N) \triangleq R^T(s)\Big|_{\epsilon^{sT/N}\to z} \tag{5}$$

Hence it is simpler to think of frequency response of discretely excited continuous systems in terms of s rather than z. Where no confusion may arise, the variables s and z may be omitted to give versatility to the notation. For the sake of notational brevity, in the following development G(s)M(s) will be written as GM(s), for occasions where s needs to be substituted by a string of notations.

The steady-state component in the sampled output is of interest. In taking the partial fraction expansion of the right-hand side of (1), one may note that the N principal roots of $z^N - \varepsilon^{jbT}$ are

$$\varepsilon^{j\frac{bT}{N}}, \quad \varepsilon^{j\frac{bT-2\pi}{N}}, \quad \varepsilon^{j\frac{bT+2\pi}{N}}, \quad \varepsilon^{j\frac{bT-4\pi}{N}}, \ldots$$

Hence the partial fraction expansion of $\frac{1}{z}C^{T/N}(z)$ may be written as

$$\frac{1}{z}C^{T/N}(z) = \sum_{n=n_1}^{n_2} \frac{A_n + jB_n}{z - \varepsilon^{j\omega_n T/N}} + [\text{terms due to modes of } (GM)^{T/N}] \tag{6}$$

where

$$\omega_n = b + \frac{2\pi n}{T}$$

$$\left.\begin{aligned} n_1 &= \tfrac{-1}{2}(N-1) \\ n_2 &= \tfrac{1}{2}(N-1) \end{aligned}\right\} \text{ if } N = \text{odd} \qquad \left.\begin{aligned} n_1 &= \tfrac{-N}{2} \\ n_2 &= \tfrac{N}{2} - 1 \end{aligned}\right\} \text{ if } N = \text{even}$$

and

$$A_n + jB_n = \left.\frac{(GM)^{T/N} z^{N-1}}{\frac{d}{dz}(z^N - \varepsilon^{jbT})}\right|_{z=\varepsilon^{j\omega_n T/N}} = \left.\frac{1}{N}(GM)^{T/N}\right|_{z=\varepsilon^{j\omega_n T/N}}$$

$$= \left.\frac{1}{N}(GM(s))^{T/N}\right|_{s=j\omega_n} \tag{7}$$

The steady-state response to ε^{jbt} can be written by inspection of (6) as

$$[c_{ss}(t)]^{T/N} = \left[\sum_{n=n_1}^{n_2} (A_n + jB_n)\varepsilon^{j\omega_n t}\right]^{T/N} \tag{8}$$

Since the system of Fig. 1 is linear the response to the imaginary part of ϵ^{jbt} is the imaginary part of the response to ϵ^{jbt}. Hence the steady-state response to $\sin bt$ is

$$[c_{ss}(t)]^{T/N} = \left[\sum_{n=n_1}^{n_2} (A_n \sin \omega_n t + B_n \cos \omega_n t)\right]^{T/N} \tag{9}$$

where A_n and B_n are determined by (7). Note the simplicity of the derivation as compared to that of Reference [1]. The difference between (9) and the corresponding expression (Eq. (11) of Reference [1]) is that, in the right-hand side of (9), the N spectral components are selected alternately between negative (subalias) and positive aliases, while only positive aliases are used in Eq. (11) of Reference [1]. It is worth noting that while both results are correct for the representation of sampled steady-state output, difficulty arises (and was overlooked) in considering the limit case of $N \to \infty$ in Eq. (11) of Reference [1]. By letting $N \to \infty$ in (9), this difficulty is circumvented. The following development demonstrates this point. The correct expression resulting from taking $N \to \infty$ in (9) is presented first.

Letting $N \to \infty$ in (9) gives

$$c_{ss}(t) = \sum_{n=-\infty}^{\infty} (A_n \sin \omega_n t + B_n \cos \omega_n t) \tag{10}$$

where, on account of (7),

$$A_n + B_n = \frac{1}{T} \lim_{n\to\infty} \frac{T}{N}(GM)^{T/N}\Big|_{s=j\omega_n}$$

$$= \frac{1}{T} \lim_{N\to\infty} \sum_{k=-\infty}^{\infty} GM(s + j\frac{2\pi kN}{T})\Big|_{s=j\omega_n} \tag{11}$$

As long as $-\frac{N}{2} \le n_1 \le n \le n_2 < \frac{N}{2}$ and $N \to \infty$, only the k=0 term contributes to the infinite sum in the right-hand side of (11) since GM(s) is always a low-pass filter. Hence, as $N \to \infty$,

$$A_n + jB_n = \frac{1}{T} GM(j\omega_n) \tag{12}$$

However, the above limit case is not true if $n = N-i$, for finite integer i. In that case,

$$A_n + jB_n = \frac{1}{T} \lim_{N\to\infty} \sum_{k=-\infty}^{\infty} GM(s - j\frac{2\pi kN}{T}) \Big|_{s=j\omega_n}$$

$$= \frac{1}{T} \lim_{N\to\infty} \sum_{k=-\infty}^{\infty} GM[j(b + \frac{2\pi(n-kN)}{T})]$$

$$= \frac{1}{T} \lim_{N\to\infty} \sum_{k=-\infty}^{\infty} GM[j(b - \frac{2\pi i}{T}) - j\frac{2\pi(k-1)N}{T}] \tag{13}$$

Now as $N \to \infty$, only the k=1 term contributes to the infinite sum in the right-hand side of (13) since GM(s) is always a low-pass filter. Thus for $n = N-i$, $N \to \infty$, finite i,

$$A_n + jB_n = \frac{1}{T} GM[j(b - \frac{2\pi i}{T})] \tag{14}$$

which is a subalias component, is not negligible, and is not represented by (12). Since the summation in Eq. (11) of Reference [1] runs between n=0 and $n = N-1$, letting $N \to \infty$ results in an A_n+jB_n which cannot be represented by (12), which is Eq. (18) of Reference [1].

A numerical example demonstrating the representation of the spectral components of the continuous output and the sampled output on a Bode-plot and an even-scaled frequency response plot, respectively,

has been given in Reference [1]. The modification and correction made in this paper requires the inclusion of subaliases or negative aliases on the frequency response plots in accordance with (8) and (10). To avoid duplication, numerical examples will not be given here. The reader is urged to apply this modification to the example given in Reference [1].

III. DIRECT DERIVATION OF THE FREQUENCY SPECTRUM OF THE CONTINUOUS OUTPUT

In the above development, the continuous output is treated as a limit case of sampled output with an arbitrarily large sampling frequency, and the infinite frequency spectrum of the continuous output is given by (10) with the spectral components A_n+jB_n given by (12). In this section, it will be shown that the frequency spectrum of the continuous output of a discretely excited continuous system can also be derived directly without invoking the sampled output. Thus it confirms the result of the previous section.

Again consider the system of Fig. 1, where

$$C(s) = G(s)M(s)R^T(s) \tag{15}$$

Let

$$g_m(t) \triangleq L^{-1}[G(s)M(s)] \tag{16}$$

Let the input be ϵ^{jbt}, with t extending from $-\infty$ to ∞. Then the steady-state response of the system may be written as

$$c_{ss}(t) = \left[\epsilon^{jbt}\right]^T * g_m(t) \tag{17}$$

where the * denotes convolution, and

$$\left[\varepsilon^{jbt}\right]^T = \varepsilon^{jbt} \sum_{n=-\infty}^{\infty} \delta(t-nT) = \frac{1}{T}\varepsilon^{jbt} \sum_{n=-\infty}^{\infty} \varepsilon^{j\frac{2\pi n}{T}t} \tag{18}$$

The last identity can be found in textbooks on Fourier series and Fourier transform [2]. Fourier transformation of (18) gives

$$F\left[\left(\varepsilon^{jbt}\right)^T\right] = \frac{2\pi}{T} \sum_{n=-\infty}^{\infty} \delta(\omega - b - \frac{2\pi n}{T}) \tag{19}$$

Fourier transform of (17) is

$$C_{ss}(j\omega) = \frac{2\pi}{T} \sum_{n=-\infty}^{\infty} \delta(\omega - b - \frac{2\pi n}{T}) G(j\omega)M(j\omega) \tag{20}$$

since $g_m(t)$ is a causal function. Now the steady-state output is obtained by inverse transforming (20):

$$c_{ss}(t) = \frac{1}{T} \sum_{n=-\infty}^{\infty} GM[j(b + \frac{2\pi n}{T})]\ \varepsilon^{j(b+\frac{2\pi n}{T})t} \tag{21}$$

Since $\omega_n = b + \frac{2\pi n}{T}$, substituting (12) into (21) gives

$$c_{ss}(t) = \sum_{n=-\infty}^{\infty} (A_n + jB_n)\ \varepsilon^{j\omega_n t} \tag{22}$$

as the steady-state response to ε^{jbt}. Note that (22) is the limit case of (8) when $N \to \infty$. Again, by virtue of the linearity of the system, (22) implies that the steady-state response to $\sin bt$ is given by (10), with $A_n + jB_n$ given by (12). In summary, the analogy between the frequency response of a continuous system and that of a discretely excited continuous system is readily demonstrated by comparing Fig. 2 and Fig. 3.

Note especially that if all the variables are represented in the s-domain, a unified concept of frequency response may be readily applied to both continuously excited and discretely excited continuous systems.

IV. CLOSED-LOOP DIGITAL CONTROL SYSTEMS

It is readily seen that if, in Fig. 2,

$$F(s) = GM\left[1 + G_1^T(G_2GM)^T\right]^{-1} G_1^T \tag{23}$$

then Fig. 2 represents the closed-loop system of Fig. 4. Since $\omega_n = b + \frac{2\pi n}{T}$ and the Laplace transform of a sampled function is periodic in s with period $j\frac{2\pi}{T}$, substituting $s=j\omega_n$ into F(s) gives

$$F(j\omega_n) = GM(j\omega_n)\left\{\left[1 + G_1^T(G_2GM)^T\right]^{-1} G_1^T\right\}_{s=jb} \tag{24}$$

The concept of frequency response set forth in Fig. 2 implies that, for the continuous output of the closed-loop system of Fig. 4,

$$A_n + jB_n = \frac{1}{T}GM(j\omega_n)\left\{\left[1 + G_1^T(G_2GM)^T\right]^{-1} G_1^T\right\}_{s=jb} \tag{25}$$

For the sampled output with sampling period T/N, the spectral components are given by substituting the right-hand side of (23) for GM in (7). Thus

$$A_n + jB_n = \frac{1}{N}\left\{GM\left[1 + G_1^T(G_2GM)^T\right]^{-1} G_1^T\right\}_{s=j\omega_n}^{T/N} \tag{26}$$

Applying multirate sampling theory (Appendix of [1]) and property of periodicity to (26) gives

$$A_n + jB_n = \left[\frac{1}{N}(GM)^{T/N}\right]_{s=j\omega_n} \left\{\left[1 + G_1^T(G_2GM)^T\right]^{-1} G_1^T\right\}_{s=jb} \quad (27)$$

Thus the spectral representation of a closed-loop discretely excited continuous system is readily obtained via the unified concept of frequency response.

V. CONCLUSIONS

This paper corrects the mistake made in a previous paper and further advances the concept of frequency response of discretely excited continuous systems. If a continuous system has transfer function F(s) and its input is R(s), then its steady-state response to $r(t)=\varepsilon^{jbt}$ is $c_{ss}(t)=F(jb)\varepsilon^{jbt}$ (Fig. 3). If R(s) is sampled and then input into F(s), then the input to the continuous system F(s) is (Fig. 2)

$$R^T(s) = \frac{1}{T}\sum_{n=-\infty}^{\infty} R(s+j\frac{2\pi n}{T}) \quad (28)$$

and the steady-state response of the discretely excited system to $r(t)=\varepsilon^{jbt}$ is

$$c_{ss}(t) = \frac{1}{T}\sum_{n=-\infty}^{\infty} F[j(b+\frac{2\pi n}{T})]\ \varepsilon^{j(b+\frac{2\pi n}{T})} \quad (29)$$

The analogy between the frequency response of a continuous system and that of a discretely excited continuous system is interesting in the sense that it enables one to write the frequency response of the latter on the basis of what is already known about the former. This unified concept of frequency response is independent of system configurations, as F(s) may represent closed-loop as well as open-loop systems.

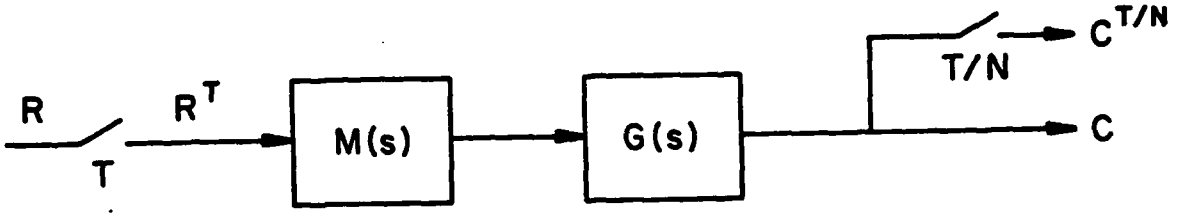

Fig. I Discretely Excited Continuous System

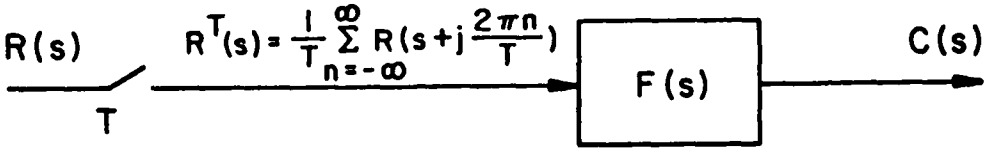

$$\text{If } r(t) = \epsilon^{jbt} \text{ Then } C_{ss}(t) = \frac{1}{T}\sum_{n=-\infty}^{\infty} F\left[j(b+\frac{2\pi n}{T})\right]\epsilon^{j(b+\frac{2\pi n}{T})t}$$

Fig. 2 Frequency Response of Discretely Excited Continuous System

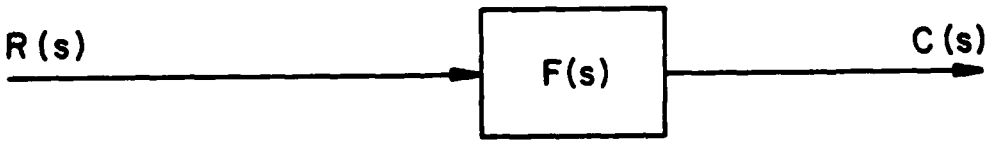

$$\text{If } r(t) = \epsilon^{jbt} \text{ Then } C_{ss}(t) = F(jb)\,\epsilon^{jbt}$$

Fig. 3 Frequency Response of Continuous System

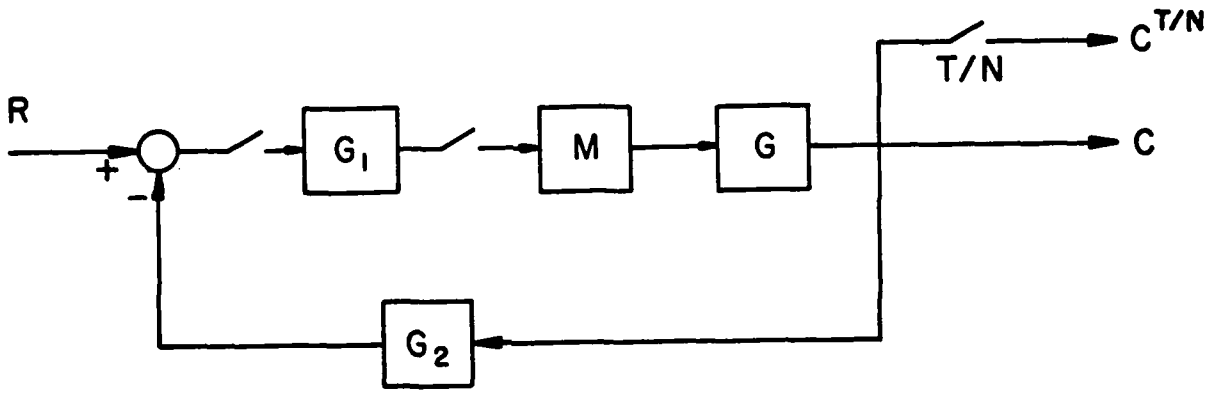

Fig. 4 A Closed-Loop Digital Control System

REFERENCES FOR APPENDIX D

[1] Whitbeck, Didaleusky and Hofmann: "Frequency Response of Digitally Controlled Systems," J. of Guidance and Control, Vol. 4, No. 4, July - August 1981, pp. 423-427.

[2] McGillem, C. D. and Cooper, G. R.: Continuous and Discrete Signal Analysis, Holt, Rinehart and Winston, 1974, p. 158.

[3] Ragazzini, J. R. and Franklin, G. F.: Sampled-data Control Systems, McGraw-Hill, 1958.

END

DATE
FILMED

7-83

DTIC